A. Hvatov

Torque Vibration Isolatior

masters project
part I

AALBORG UNIVERSITET
2015

Title: Torque vibration isolator

Theme: Engineering Design of Mechanical Systems Master's Project

Project period(first part):
01/09-2015 - 18/12-2015

Project group:
3.223

Author:

Alexandr Hvatov

Supervisor:
Sergei Sorokin

AALBORG UNIVERSITY
STUDENT REPORT
Department of Mechanical and Manufacturing Engineering
Fibigerstraede 16
DK 9220 Aalborg Oest
Tlf. 9940 9297
Fax 9815 1675
Web www.ses.aau.dk

Synopsis:

First part of this Master project contains preliminary consideration of the circular membrane in polar coordinates which will be used in second part of project, where thin plate-cylindrical shell model considered. Also curved beam model of vibration torque isolator considered. Torque isolation modelled as series of periodic alternating Bernoulli-Euler. In order to obtain solution Floquet theory used. Analytical solution was obtained by using of boundary integrals method, Green's matrix was derived using bi-orthogonality conditions.

No. printed Copies: 4

No. of Appendix Pages: 11

Completed: 18/12-2015

Table of contents

Introduction

In many industrial applications it is necessary to isolate components from vibration in connected neighbour components. This is also the case for various rotational transmission systems. It has been shown for different applications see e.g. [1–8], that periodic structures can generate such a vibration isolation. An idea for such a torque vibration isolator consisted of periodically repeated substructures with sufficient static torque stiffness, is sketched here below in Fig.1:

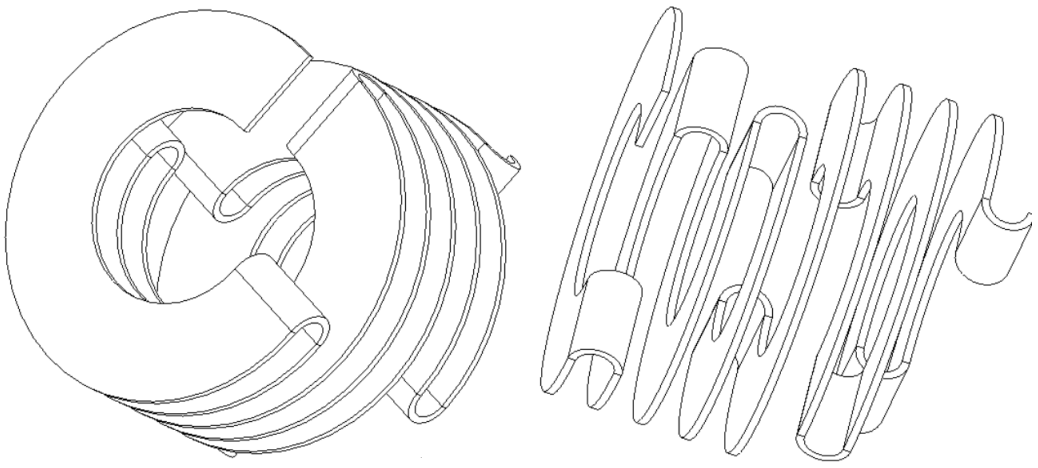

Figure 1: Vibration isolator sketch

Main idea of project is to model vibration isolator sketched above in order to have the main advantages and disadvantages being seen before experiments are conducted. Also should be considered general possibility of construction vibration isolation torque sketched above and how this kind of structure affects on power flow from a wind turbine generator should be explored.

Models, considered in this work are based on differential equations and in order to find solution of these equations following instruments are used:

1.Boundary Integral Equations method is used to find solution of a differential equation, using only information about function and its derivatives on the boundary of volume considered in given problem. In this method Green's matrices are commonly used, which are solution of equation with point force excitation. And in this work, bi-orthogonality conditions (in this work they are used without detail explanation, because this theory lies out of scope of this work, more detailed description can be found in [9]) are employed to find Green's matrices. In appendix C, application of this method to a simple case of axial rod vibrations is shown.

2. Floquet theory is widely used in order to obtain solution for periodically alternating infinite structures. As shown for example in [7, 8] infinite structure cases are in good correspondence with a finite one and therefore Floquet theory gives good possibility to analyse periodic structures and understand mechanisms of wave propagation in periodic structures. In appendix D, application of this method to a simple case of axial rod vibrations is shown.

Goal of this work is to model vibrational isolation torque as a periodical structure and provide experimental data in order to see quality of modelling. All work divided in following subtasks:

(I) Show possibility of using Floquet theory in polar coordinates on example of circular membrane equation, since isolator, shown on a Fig.1 contains part, that is modelled as a part of the circular plate, which equation is naturally written in polar coordinate system. Floquet theory is well studied in cartesian coordinate system [1], but there are no works, where application of Floquet theory to other coordinate systems is shown.

(II) Derivation and evaluation of boundary integral equations for a beam model (first model), based on Bernoulli-Euler flat ring equations

(III) Derivation and evaluation of boundary integral equations for a Kirchoff-Love plate and cylindricall shell model (second model) with use of polar coordinates

(IV) Experimental validation of first and second model

Since it is a long master's project in first part only subtasks (I) (Ch.2) and (II) (Ch.3) are considered. Parts (III) and (IV) will be covered in second part of project.

Project is written in comprehensive way and information in appendix can be used as supply for more clear understanding of methods, that lies in ground of this project. Information in appendices is not mandatory for understanding ideas of this project.

Chapter 1

The concept of a periodic structures

Here common definitions for all periodic structures considered in this work are introduced. First, an infinite periodic structure as shown on Fig.1.1 can be considered:

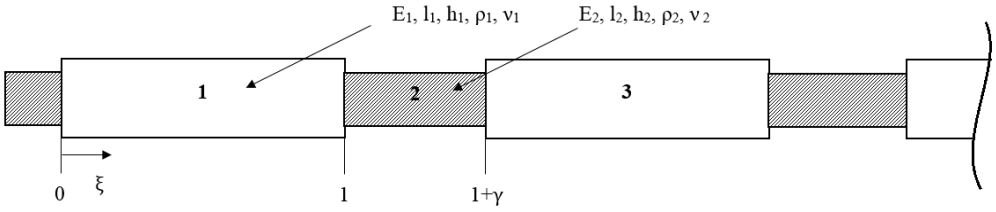

Figure 1.1: Infinite periodical structure scheme

,where ξ is the common coordinate (axial coordinate of bar, radial coordinate of a circular membrane, natural coordinate of spring). Each component of a periodic structure can have different material parameters (like Young modulus), shape parameters (like curvature) and length repeating in periodic alternating manner. In order to use Floquet theory at least one parameter excluding length should be different for two segments. In terms of vibrations, different wavenumbers k_i for each part are required.

The existence of frequency stop- and pass-bands in infinite periodic waveguides is well known and understood since the pioneering work by L.Brillouin [1]. The vibro-acoustics of beams, plates and shells and pipes with periodic attachments or step-wise varying properties has been broadly explored by many authors. Classial works [1, 2] and the modern one [3–8] are just a few of those, which illustrate the classical and recent advances in this area of research and that it is of interest to develop methods for various waveguides and make industrial application of theory of periodic structures.

Infinite structure can be considered as built from finite structures called periodicity cell. Here only periodicity cell with one period length are considered. Periodicity cells can be chosen arbitrary, for example as:

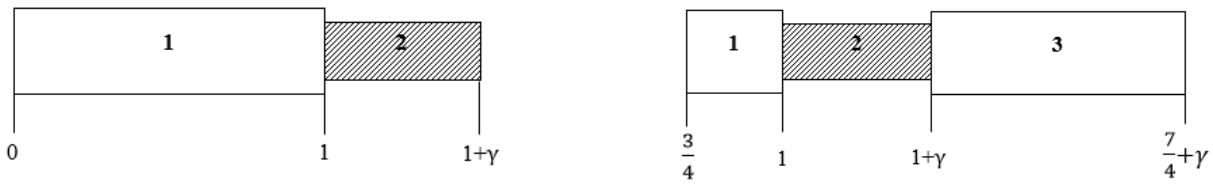

Figure 1.2: Different periodicity cells schemes

But most interesting properties are of a cell, which can be schematically illustrated as:

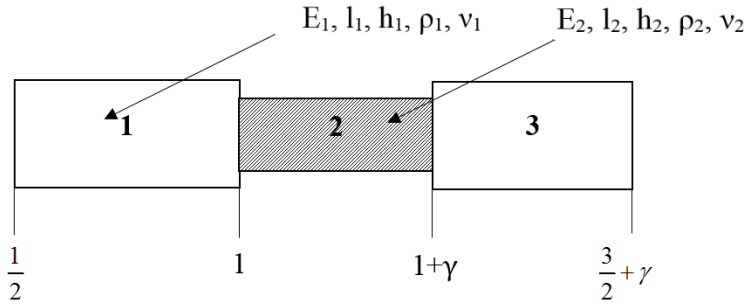

Figure 1.3: Symmetrical periodicity cell scheme

Structure, illustrated on Fig.1.3 called symmetrical periodicity cell (half "white"part - "black"part half "white"part) and it has some important properties: it has one period length $1 + \gamma$ and it is balanced with respect to center of masses, i.e. geometrical and gravity centers are in same point.

Since infinite structure can not be implemented practically, one can consider also a finite structures, built from symmetrical cells. This kind of finite structures has some interesting properties, which will be described in next chapters. One can consider non-symmetrical cell as a 'building block' but it does not have such properties and will not be considered in this work.

Properties of a finite and infinite structure are closely related to each other, and therefore both structures can be considered simultaneously in order to show full picture of wave propagation and vibrations.

Chapter 2

Periodic circular membrane

Torque vibration isolator shown on Fig.1 can be considered as an ensemble of flat ring plates and cylindrical shells, connected in an alternative manner, i.e. as a periodic structure. Equation of motion of flat ring plate is naturally written in the polar coordinate system. Therefore, it is expedient to investigate performance of a periodic structure in polar coordinates. Previously in [7] and [8] most simple cases of axial and flexural vibrations of periodic beams and vibrations of cylindrical shell were considered. Main ideas of these articles were shown for cartesian coordinate system. Main goal of this chapter is to consider different coordinate system and show that all properties of the periodic structures for cartesian coordinates are preserved in polar coordinate system with simple circular membrane as an illustrative example.

2.1 Membrane vibration equation. Green's function.

General equation of motion for the membrane has the form (see App.A for derivation from Hamilton's principle and [10]):

$$\left(\Delta + k^2\right) u = u_{rr} + \frac{1}{r}u_r + \frac{1}{r^2}u_{\varphi\varphi} + k^2 u = -q(r,\varphi) \tag{2.1}$$

,where $q(r,\varphi)$ is the intensity of distributed force.
The external force can be presented as:

$$q\left(r,\varphi\right) = \sum_{m=0}^{+\infty} Q_m(r)\cos(m\varphi) \tag{2.2}$$

Then general solution can also be expanded in Fourier series :

$$u\left(r,\varphi\right) = \sum_{m=0}^{+\infty} U_m(r)\cos(m\varphi) \tag{2.3}$$

Which substituted into Eq.2.1 gives:

$$\left(\Delta + k^2\right) u = \sum_{m=0}^{+\infty}\left(\frac{\partial^2 U_m(r)}{\partial r^2} + \frac{1}{r}\frac{\partial U_m(r)}{\partial r} + (k^2 - \frac{m^2}{r^2})U_m(r)\right)\cos(m\varphi) = -\sum_{m=0}^{+\infty} Q_m(r)\cos(m\varphi) \tag{2.4}$$

Since $\cos m\phi$ are independent functions, for each circumferential wave number m decoupled equation can be solved (hereafter, index m is omitted in all equations):

$$U''(r) + \frac{1}{r}U'(r) + \left(k^2 - \frac{m^2}{r^2}\right)U(r) = -Q(r) \tag{2.5}$$

In order to obtain solution Green's function method is used. By definition [11], Green's function is a solution of the equation (in what follows $\frac{\partial}{\partial r}G(r,r_0) = G'(r,r_0)$):

$$G''(r,r_0) + \frac{1}{r}G'(r,r_0) + \left(k^2 - \frac{m^2}{r^2}\right)G(r,r_0) = -\delta(r-r_0) \tag{2.6}$$

,where $\delta(x)$- Dirac delta function. Here delta function $\delta(r-r_0)$ has meaning of intensity of point force, applied at the point r_0 and distributed in the angular coordinate direction as $\cos(m\varphi)$, and r is the observation point. Therefore second derivative $G''(r,r_0)$ has dimension of force intensity

Green's function of an ordinary second-order differential equation has a following properties [11] (for clarity notation of point of excitation and observation preserved).

Symmetry with respect to observation and excitation point property:

$$G(r,r_0) = G(r_0,r) \tag{2.7a}$$

Unit jump in derivative at the excitation point:

$$\frac{\partial}{\partial r}G(r_0,r_0+\varepsilon) - \frac{\partial}{\partial r}G(r_0,r_0-\varepsilon) = 1,\ \varepsilon \to 0 \tag{2.7b}$$

Continuity at the excitation point:

$$G(r_0,r_0+\varepsilon) = G(r_0,r_0-\varepsilon),\ \varepsilon \to 0 \tag{2.7c}$$

It should be noted that ,since second derivative $G''(r,r_0)$ has dimension of force intensity, $\frac{\partial}{\partial r}G(r,r_0)$ in this case has dimension of the force, acting on a radial direction. Therefore, force should have unit jump at the coordinate $r = r_0$. Also, property of unit jump is a reflection of mathematical theorem $\frac{d}{dx}\theta(x) = \delta(x)$, where $\theta(x)$ is the Heaviside theta-function. As known, theta-function has unit jump at the point $x = 0$.

Last two properties Eq.2.7b-Eq.2.7c can be used for obtaining explicit form of Green's function of equation Eq.2.5. The general solution of equation Eq.2.6 with arbitrary excitation point r_0 has a form:

$$\begin{aligned} u_+(r) &= A\ H_m^{(1)}(kr)\,, r > r_0 \\ u_-(r) &= B\ H_m^{(2)}(kr)\,, r \le r_0 \end{aligned} \tag{2.7}$$

, where $H_m^{(1)}(r)$ and $H_m^{(2)}(r)$ are Hankel's functions of order m of first and second kind respectively and A, B are integration constants.

In order to consider infinite structures function $u_+(r)$ should satisfy radiation, or Sommerfeld, condition [12].

With properties Eq.2.7a-Eq.2.7c one can obtain system of linear algebraical equations with respect to constants A, B:

$$\begin{aligned} &u_+(r_0) = u_-(r_0) \\ &\tfrac{d}{dr}u_+(r_0) - \tfrac{d}{dr}u_-(r_0) = 1 \end{aligned} \tag{2.8}$$

Constants are found as:

$$\begin{aligned} A &= -\frac{H_m^{(2)}(k\,r_0)}{k(H_{m+1}^{(1)}(k\,r_0)H_m^{(2)}(k\,r_0) - H_{m+1}^{(2)}(k\,r_0)H_m^{(1)}(k\,r_0))} = -\tfrac{1}{4}i\pi r_0 H_m^{(2)}(k\,r_0) \\ B &= -\frac{H_m^{(1)}(k\,r_0)}{k(H_{m+1}^{(1)}(k\,r_0)H_m^{(2)}(k\,r_0) - H_{m+1}^{(2)}(k\,r_0)H_m^{(1)}(k\,r_0))} = -\tfrac{1}{4}i\pi r_0 H_m^{(1)}(k\,r_0) \end{aligned} \tag{2.9}$$

Thus, Green's function for equation 2.5 have form:

$$G(r,r_0)=\begin{cases}-\frac{1}{4}i\pi r_0 H_m^{(1)}(k\,r_0)H_m^{(2)}(k\,r) & r\le r_0\\ -\frac{1}{4}i\pi r_0 H_m^{(2)}(k\,r_0)H_m^{(1)}(k\,r) & r>r_0\end{cases} \tag{2.10}$$

It should be noted, that this form of Green's function in not unique. One can choose an arbitrary combination of Bessel functions $Y(r)$ and $J(r)$ as the general solution Eq.2.7. Also, any solution of the homogenous equation Eq.2.5 (with $Q(r)\equiv 0$) can be added to the existing form of a Green's function.

It is convenient to define Green's function as a solution of the equation (for more detailed explanation see App.B):

$$G''(r,r_0)+\frac{1}{r}G'(r,r_0)+\left(k^2-\frac{m^2}{r^2}\right)G(r,r_0)=-\frac{\delta(r-r_0)}{r_0} \tag{2.6'}$$

From physical point of view, with this definition force resultant $F=\int_0^{2\pi}\int_a^b -\frac{\delta(r-r_0)}{r_0}rdrd\phi=-\frac{2\pi}{r_0}\int_a^b\delta(r-r_0)rdr=-\frac{2\pi r_0}{r_0}=-2\pi$ remains constant when point of excitation r_0 is changing.

With definition 2.6' Green's function has form:

$$G(r,r_0)=\begin{cases}-\frac{1}{2}i\pi H_m^{(1)}(k\,r_0)H_m^{(2)}(k\,r) & r\le r_0\\ -\frac{1}{2}i\pi H_m^{(2)}(k\,r_0)H_m^{(1)}(k\,r) & r>r_0\end{cases} \tag{2.11}$$

One can plot real part of function 2.11 in order to see that all properties of Green's function are present and Green's function was found correctly. Let $k\equiv 1$ and $r_0=1$ therefore jump at the point $r=1$ of the function $G'(r,r_0)$ should be $\frac{1}{r_0}=1$:

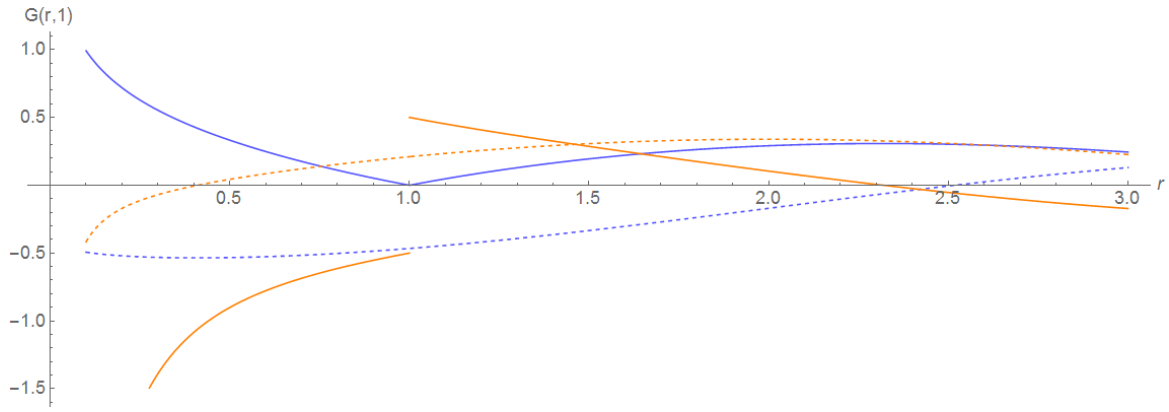

Figure 2.1: Functions G (blue) and G'(orange) for $r_0=1$, dashed - imaginary part

As seen, function $G(r,1)$ is continuous at point $r=1$, but function $G'(r,1)$ experience unit jump, as were predicted. Imaginary part is continuous in both cases, it does not affect unit jump.

Dirac's delta function $\delta(r)$ has remarkable property (which in mathematics is the definition of Dirac's delta function):

$$\int_a^b \delta(r-r_0)f(r)dr=f(r_0) \tag{2.12}$$

Eq.2.12 is valid for any interval $r_0\in(a,b)$, including $(-\infty,+\infty)$

And from equations Eq.2.5 - Eq.2.6' and property Eq.2.12 one can obtain displacement $u(r_0)$ at any excitation point r_0 for arbitrary force intensity $q(r)$ (it is shown in App.B). Displacement of a membrane has the form:

$$u(r_0) = [u'(r)G(r,r_0) - u(r)G'(r,r_0)]r\Big|_{r=a}^{r=b} + \int_a^b q(r)G(r,r_0)dr \tag{2.13}$$

Identity Eq.2.13 is a particular case of Kirchhoff integral in acoustics [12, 13].

It should be emphasized, that $G'(r,r_0)$ is not uniquely defined at $r = r_0$ and since we consider values $G'(r,r_0)$ at the boundary value taken as limit from inside of a membrane. Let $r = a, r = b$ be the membrane boundaries, then limits have form:

$$\begin{aligned} G'(a,r_0)\Big|_{r_0=a} &= G'(a,a+\varepsilon)\ ,\varepsilon \to 0 \\ G'(b,r_0)\Big|_{r_0=b} &= G'(b,b-\varepsilon)\ ,\varepsilon \to 0 \end{aligned} \tag{2.14}$$

Let us consider Eq.2.11. Using following series expansion at the point $z = 0$:

$$\begin{aligned} H_m^{(1)}(z) &= 1 + \tfrac{2i(\gamma-\log(2))}{\pi} + \tfrac{2i(\log(z))}{\pi} + O\left(z^2\right) \\ H_m^{(2)}(z) &= 1 - \tfrac{2i(\gamma-\log(2))}{\pi} - \tfrac{2i(\log(z))}{\pi} + O\left(z^2\right) \end{aligned} \tag{2.15}$$

,where $\gamma \approx 0.577216$ is the Euler-Mascheroni constaint.

With this Eq.2.11 to the leading order can be rewritten as:

$$G(r,r_0) = \begin{cases} \frac{1}{2\pi}\left(-2i\log\left(\frac{kr}{2}\right) + \pi - 2i\gamma\right)\left(2\log\left(\frac{kr_0}{2}\right) - i\pi + 2\gamma\right) & r \le r_0 \\ \frac{1}{2\pi}\left(2\log\left(\frac{kr}{2}\right) - i\pi + 2\gamma\right)\left(-2i\log\left(\frac{kr_0}{2}\right) + \pi - 2i\gamma\right) & r > r_0 \end{cases} \tag{2.16}$$

With derivative taken:

$$\frac{d}{dr}G(r,r_0) = \begin{cases} -\frac{i}{\pi r}\left(2\log\left(\frac{kr_0}{2}\right) - i\pi + 2\gamma\right) & r \le r_0 \\ \frac{i}{\pi r}\left(-2\log\left(\frac{kr_0}{2}\right) + \pi - 2i\gamma\right) & r > r_0 \end{cases} \tag{2.17}$$

If we find Green's function value at point $r = r_0 + \varepsilon$

$$\frac{d}{dr}G(r_0+\varepsilon,r_0) = -\frac{2i\log(k(r_0+\epsilon)) + \pi + 2i\gamma - i\log(4)}{\pi r_0} \tag{2.18}$$

If $\varepsilon = 0$ then $\frac{d}{dr}G(r_0,r_0) = -\frac{1}{r_0} - \frac{2i\log(kr_0)}{\pi r_0} - \frac{2i\gamma}{\pi r_0} + \frac{i\log(4)}{\pi r_0}$. After same procedure repeated for $r = r_0 - \varepsilon$ gives $\frac{d}{dr}G(r_0,r_0) = \frac{1}{r_0} - \frac{2i\log(kr_0)}{\pi r_0} - \frac{2i\gamma}{\pi r_0} + \frac{i\log(4)}{\pi r_0}$. Thus we obtain value for Green's function at the point $r = r_0$ and this value depends on a limit direction.

$$\frac{d}{dr}G(r_0 \pm \varepsilon, r_0) = \mp\frac{1}{r_0} - \frac{2i\log(kr_0)}{\pi r_0} - \frac{2i\gamma}{\pi r_0} + \frac{i\log(4)}{\pi r_0} \tag{2.19}$$

If more terms in the series expansion Eq.2.15 are taken, only precision of common part are increasing, $\mp\frac{1}{r_0}$ is only part that changes with change of limit direction.

In what follows, it is assumed that all limits are taken correctly for all parts of membrane. Before considering periodic structure single membrane can be considered in order to show the idea of boundary integrals equations method.

Let $r = a$ and $r = b$ be circular membrane boundaries. Thus, one writes two boundary integrals in form:

$$\begin{aligned} u(a) &= [u'(r)G(r,a) - u(r)G'(r,a)]r\Big|_{r=a}^{r=b} + \int_a^b q(r)G(r,a)dr \\ u(b) &= [u'(r)G(r,b) - u(r)G'(r,b)]r\Big|_{r=a}^{r=b} + \int_a^b q(r)G(r,b)dr \end{aligned} \tag{2.20}$$

Unknown here are two displacements at the boundaries $u(a), u(b)$ and two forces $u'(a), u'(b)$. In order to close system of algebraic equations two more equations should be written. For single membrane these are boundary conditions in form:

$$\begin{aligned} u(a) &= 0 \\ u(b) &= 0 \end{aligned} \tag{2.21}$$

or

$$\begin{aligned} u'(a) &= 0 \\ u'(b) &= 0 \end{aligned} \tag{2.22}$$

Mixed conditions can be stated too. Main principle is that energy functional should be minimized (see. App.A). In this work only symmetrical boundary conditions are considered.

Eq.2.20,Eq.2.21 or Eq.2.20, Eq.2.22 are four algebraical equations with respect to four unknowns $u(a), u(b), u'(a), u'(b)$ and this system has unique solution. When unknowns are found and substituted into Eq.2.13, displacement at any point inside the domain $a < r_0 < b$ can be found.

2.2 Periodic structure

2.2.1 Infinite structure

We consider periodic membrane shown on Fig.2.2:

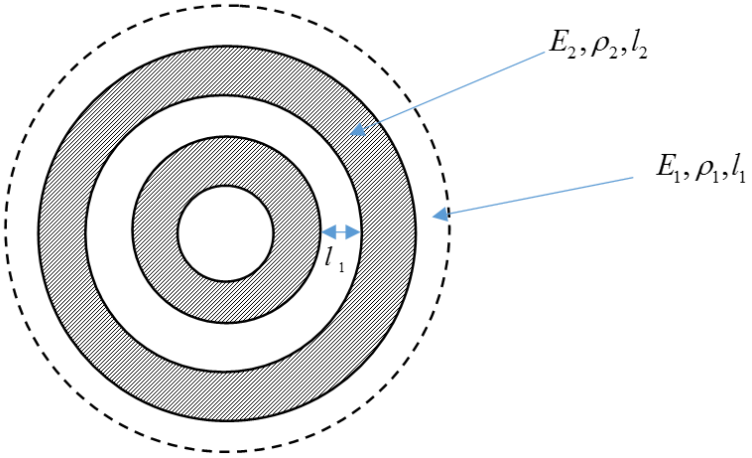

Figure 2.2: Infinite membrane scheme

Where “black” and “white” part have different material parameters: Young’s modulus, wave propagation speed and length. Following dimensionless parameters are used in this work:

$$\alpha = \frac{E_2}{E_1};\ \beta = \frac{h_2}{h_1}; \gamma = \frac{l_2}{l_1};\ \sigma = \frac{c_2}{c_1}; \lambda = \frac{l_1}{h_1}; k_1 l_1 = \Omega \tag{2.23}$$

Infinite periodical structure is considering with respect to radial coordinate r (see Fig. 1.2)

With this eigenfrequencies problem can be rewritten in terms of boundary integration equations. For each cell we write boundary equations at both ends in form:

$$\begin{aligned} u_i(a_i) &= \left[u'(r)G_i(r,a_i) - u(r)G_i'(r,a_i)\right] r\big|_{r=a_i}^{r=b_i} + \int\limits_{a_i}^{b_i} q(r)G_i(r,a_i)dr \\ u_i(b_i) &= \left[u'(r)G_i(r,b_i) - u(r)G_i'(r,b_i)\right] r\big|_{r=a_i}^{r=b_i} + \int\limits_{a_i}^{b_i} q(r)G_i(r,b_i)dr \end{aligned} \tag{2.24}$$

, where u_i are displacement, a_i are left and b_i are right boundaries of i-th part of membrane respectively. For each part we have 2 unknown displacements and 2 unknown forces at the boundaries.

In order to show main principle one periodicity cell can be considered. Since Bessel $Y(r)$ function contains singularity at point $r = 0$ the central cell, that contains point $r = 0$ should be excluded from consideration. Thus, boundary conditions have form:

$$\begin{aligned}
u_2(a_2) &= \left[u'(r)G_2(r,a_2) - u(r)G_2'(r,a_2)\right] r|_{r=a_2}^{r=b_2} + \int\limits_{a_2}^{b_2} q(r)G_2(r,a_2)dr \\
u_2(b_2) &= \left[u'(r)G_2(r,b_2) - u(r)G_2'(r,b_2)\right] r|_{r=a_2}^{r=b_2} + \int\limits_{a_2}^{b_2} q(r)G_2(r,b_2)dr \\
u_3(a_3) &= \left[u'(r)G_3(r,a_3) - u(r)G_3'(r,a_3)\right] r|_{r=a_3}^{r=b_3} + \int\limits_{a_3}^{b_3} q(r)G_3(r,a_3)dr \\
u_3(b_3) &= \left[u'(r)G_3(r,b_3) - u(r)G_3'(r,b_3)\right] r|_{r=a_3}^{r=b_3} + \int\limits_{a_3}^{b_3} q(r)G_3(r,b_3)dr
\end{aligned} \tag{2.25}$$

As seen, there are four unknown displacements $u_2(a_2), u_2(b_2), u_3(a_3), u_3(b_3)$ and four unknown forces $u_2'(a_2), u_2'(b_2), u_3'(a_3), u_3'(b_3)$. Therefore four more equations should be added. Two equations are interfacial conditions between two cells, that allows to consider cells in the system and represents continuity and forces equilibrium at the interface:

$$\begin{aligned}
u_2(b_2) &= u_3(a_3) \\
\alpha u_2'(b_2) &= u_3'(a_3)
\end{aligned} \tag{2.26}$$

And two last equations are taken from Floquet periodicity theorem. That theorem allows to close system in case of infinite structure. Any two points for Floquet conditions can be taken, but with one period distance $(1+\gamma)\lambda$ between points, i.e. $b_3 - a_2 = (1+\gamma)\lambda$:

$$\begin{aligned}
u_2(a_2) &= \Lambda u_3(b_3) \\
u_2'(a_2) &= \Lambda u_3'(b_3)
\end{aligned} \tag{2.27}$$

It should be emphasized that if one can consider first cell it is usually written as $u_1(b_1)$ instead of $u_2(a_2)$ and $u_1'(b_1)$ instead of $u_2'(a_2)$. Nevertheless, that is the same point and therefore it does not affect the solution.

Equations Eq.2.25-Eq.2.27 represent system of eight linear algebraical equations. In load-free case, i.e. when $q(r) = 0$ system is homogeneous. In order to find non-trivial solution condition $D(\Lambda, \Omega) = 0$, where $D(\Lambda, \Omega)$ is the determinant of the system Eq.2.25-Eq.2.27, must be fulfilled. In case of circular membrane $D(\Lambda, \Omega)$ is the second order polynomial in Λ and we can find its roots for each Ω and plot them as shown on Fig.2.3.

In case of cartesian coordinates $\Lambda = \exp(iK_B)$ (see [1]) and zones where $\text{abs}(\Lambda) = 1$ are called pass bands. It happens when K_B is purely real number. In this case waves can propagate freely, because magnitude of waves are not change throughout the period, changes only phase. But in case of membrane it is not obviously so, as seen on Fig.2.3 in the zones, similar to cartesian pass bands , the parameter Λ has magnitude close to 2 and it should have another form, than $\exp(iK_B)$.

At first we consider wave propagation far away from center . This case should fully correspond to axial rod vibrations case in cartesian coordinates , because following limit can be considered:

$$\left(\Delta_{polar}^{(2)} + k^2\right) u = u_{rr} + \frac{1}{r}u_r + \frac{1}{r^2}u_{\varphi\varphi} + k^2 u \;\rightarrow\; u_{rr} + k^2 u = \left(\Delta_{cartesian}^{(1)} + k^2\right) u \,, r \rightarrow \infty \tag{2.28}$$

Therefore, shape of pass- and gap-bands should repeat shape for the axial beam vibration considered in [8] and App.D.

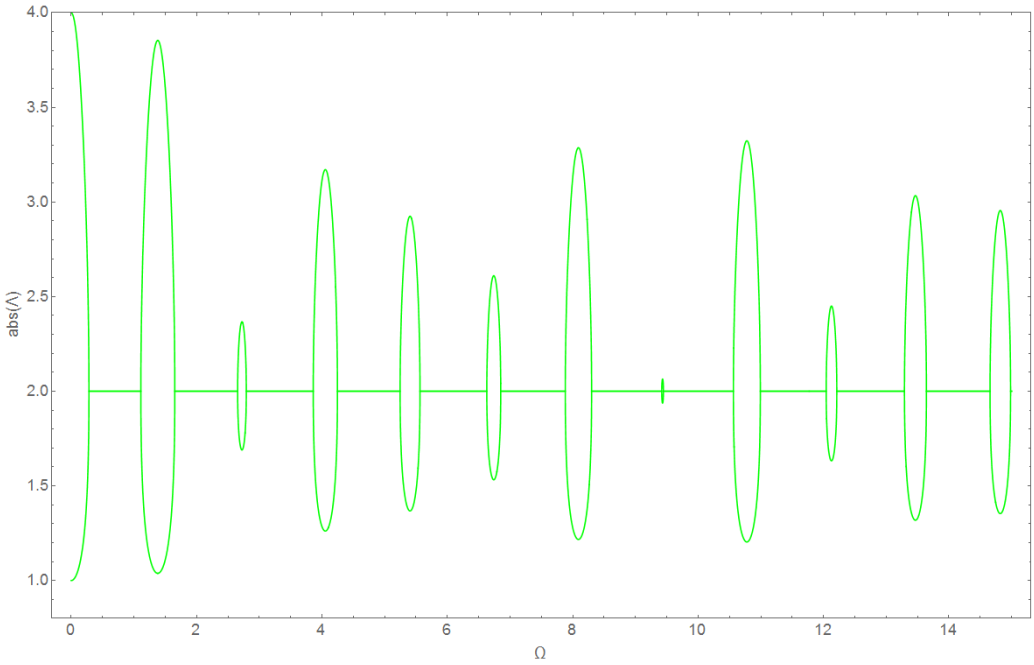

Figure 2.3: Floquet zones

In order to reach limit several consequent cells considered. Finite structure consisting of n cells is taken and then Floquet conditions used in order to transfer to infinity. Hereafter, number n is called a number of precalculated cells. Therefore, we prescribe $2n$ pair of the interfacial conditions:

$$\begin{aligned} &u_1(\lambda) = u_2(\lambda) \\ &u'_1(\lambda) = \alpha\beta u'_2(\lambda) \\ &u_2((1+\gamma)\lambda) = u_3((1+\gamma)\lambda) \\ &\alpha\beta u'_2((1+\gamma)\lambda) = u'_3((1+\gamma)\lambda) \\ &\dots \\ &u_{2n-1}(L_{2n-1}) = u_{2n}(L_{2n-1}) \\ &u'_{2n-1}(L_{2n-1}) = \alpha\beta u'_{2n}(L_{2n-1}) \end{aligned} \tag{2.29}$$

,where $L_n = ((1+\gamma)n+1)\lambda$ - distance from 0 to end of n-th periodicity cell.

And, since an infinite membrane is considered, we use Floquet conditions to transfer from n-th cell to infinity:

$$\begin{aligned} u_{2n-1}(L_{n-1}) &= \Lambda u_{2n+1}(L_{2n-1} + (1+\gamma)\lambda) \\ u'_{2n-1}(L_{n-1}) &= \Lambda u'_{2n+1}(L_{2n-1} + (1+\gamma)\lambda) \end{aligned} \tag{2.30}$$

Equations Eq.2.29-Eq.2.30 together with boundary integrals in form Eq.2.24 for each part of membrane compose the system of homogenous linear algebraical equations with respect to unknown displacements and forces at the borders and condition of non-triviality of solution can be used for finding Floquet zones. For three precalculated cells it is shown on Fig.2.4

Gap band at the proximity of $\Omega = 0$ appears due to singularity of a function $H_m^{(1)}(r)$ at the point $r = 0$. Green's function including function $H_m^{(1)}(kr)$ and wave number is function of frequency $k = k(\Omega)$. Moreover, $k(\Omega) \to 0$ when $\Omega \to 0$. Thus at the point $\Omega = 0$ argument in $H_m^{(1)}(kr)$ is zero. And therefore gap bang at proximity of the point $\Omega = 0$ can not be considered as real gap-band and waves in this frequency region have the properties of pass band waves.

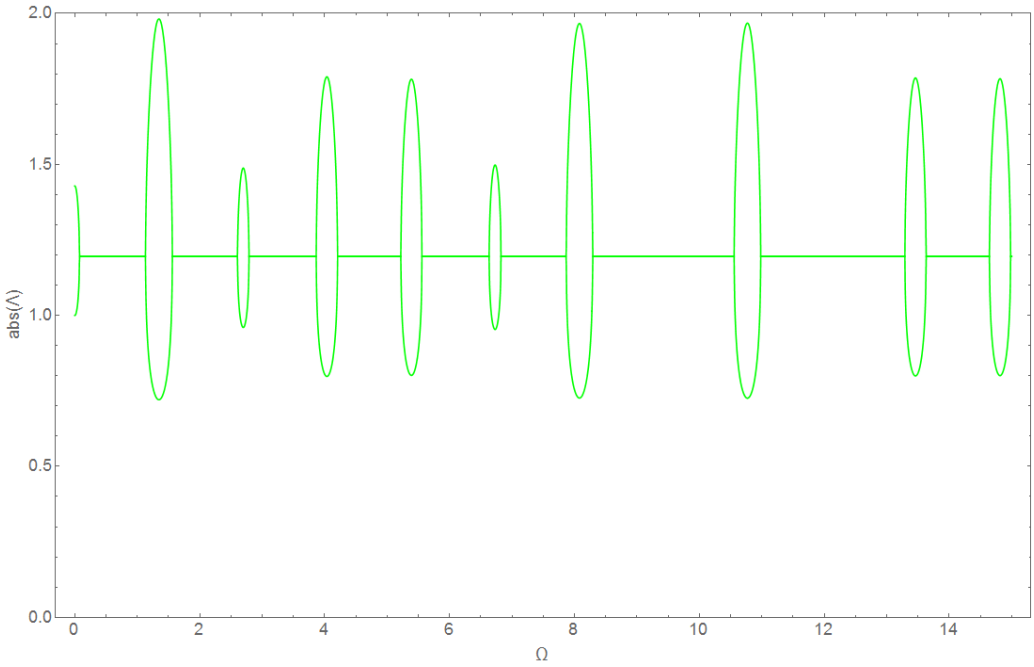

Figure 2.4: Floquet zones for n=3

The effect is vanishing when wave propagation far away from center is considered and when sufficient number of precalculated cells is taken, Floquet zones picture for circular membrane in polar coordinates fully repeats one for axial beam rod vibrations in cartesian coordinates:

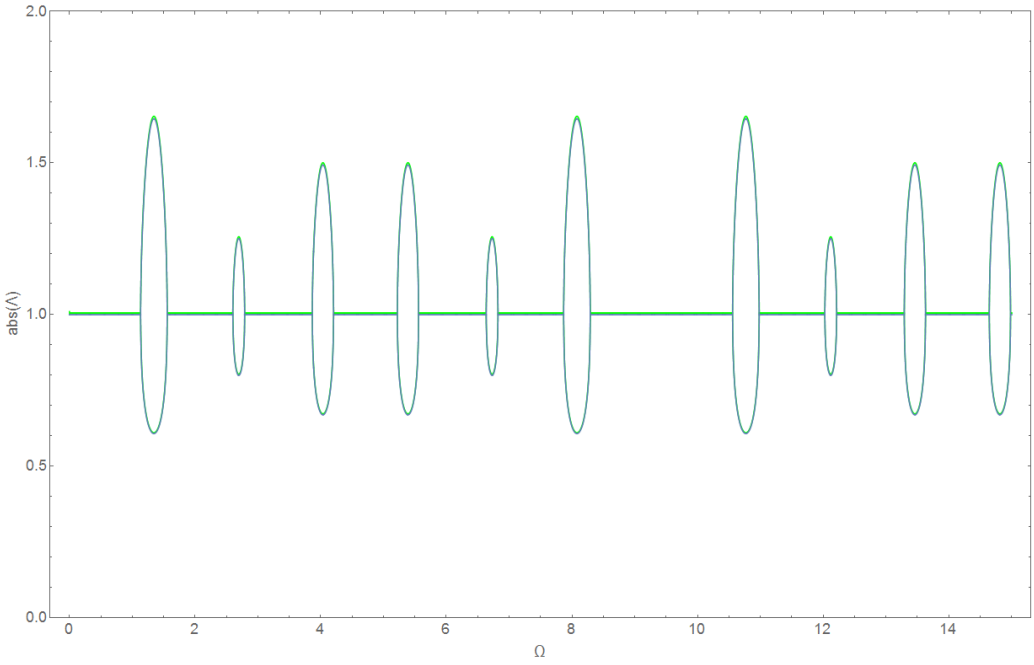

Figure 2.5: Floquet zones (axial vibrations – blue, membrane (n=100) – green)

That fact, that $abs(\Lambda) \neq 1$ even in pass bands means that $\Lambda \neq \exp(i\,K_B)$ as in cartesian coordinates case. In first model it differs and difference depends on number of pre-calculated cells. Since $\left(\Delta^{(2)}_{polar} + k^2\right) u \rightarrow \left(\Delta^{(1)}_{cartesian} + k^2\right) u$ at $r \rightarrow +\infty$ with order of $\frac{1}{r}$ then one can suppose that

$$K_B^{polar} = K_B^{cart} + \frac{1}{r_{char}}$$
$$\Lambda^{polar} = \Lambda^{cart} \exp\left(\frac{1}{r_{char}}\right) = \exp(i\, K_B) \exp\left(\frac{1}{r_{char}}\right) \tag{2.31}$$

,where $r_{char}$is a characteristic length of the model. For first model was found that $r_{char} = \frac{1}{n\gamma}$ and if corrected Floquet zones are plotted ($n = 20, m = 0$) it shows good correspondence:

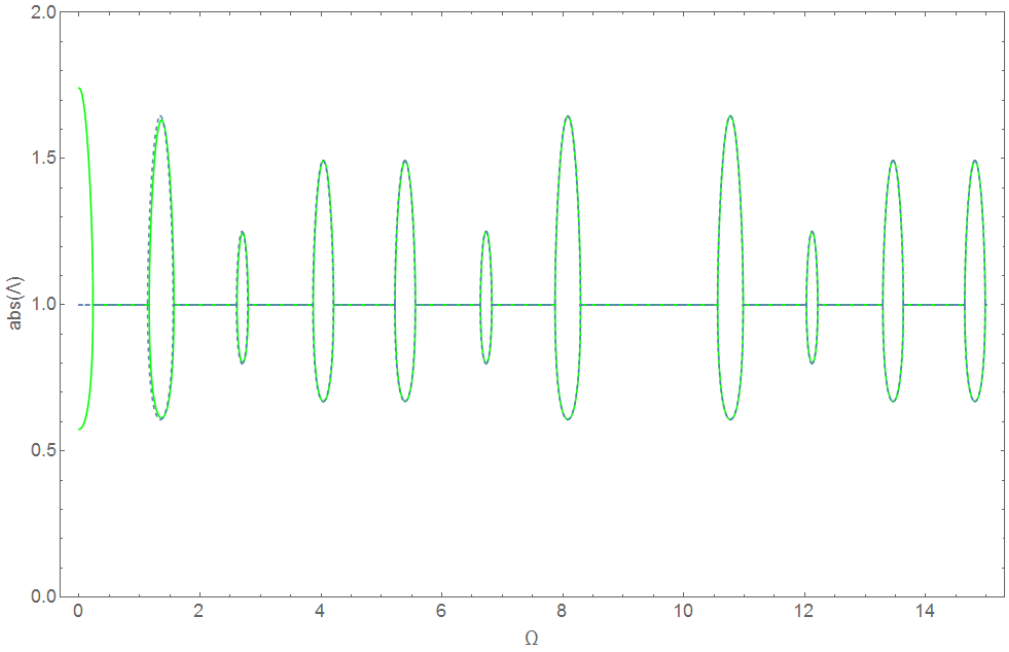

Figure 2.6: Corrected Floquet zones ($n = 20, m = 0$)

Besides number n of precalculated cells there is second parameter m – number of circumferential waves. As shown on the Fig.2.7, parameter m does not change value of $abs(\Lambda)$ for given n, it affects only on width of zero 'gap' band. With parameter m increasing increases width of zero gap band and increases difference from cartesian case in low frequency range:

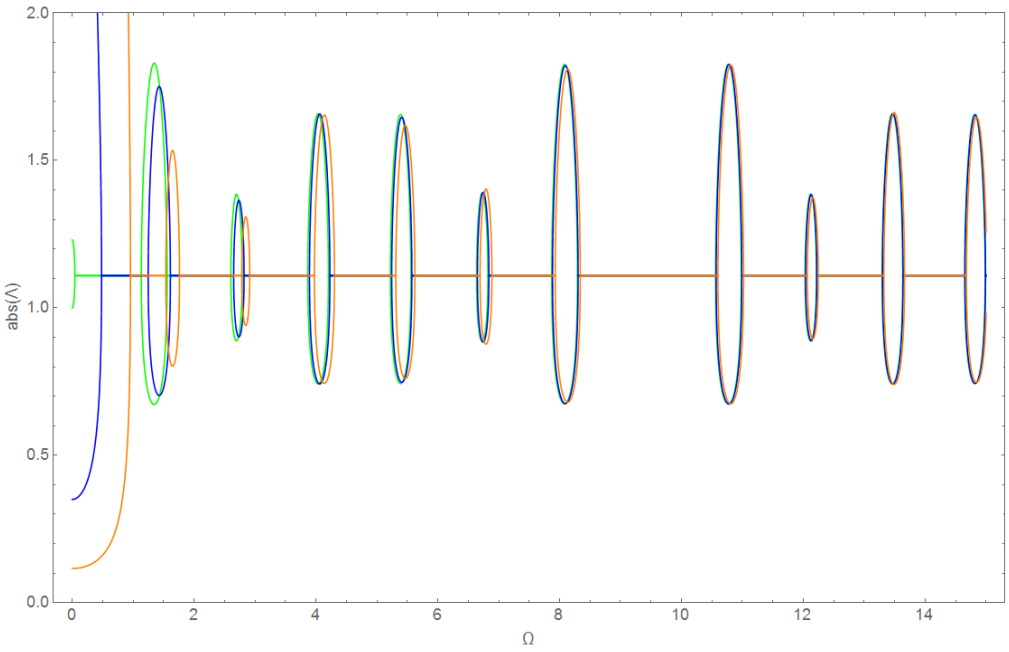

Figure 2.7: Floquet zones for n=5 and m=0 (green), m=5 (blue),m=10 (orange)

As seen, main patterns, found for cartesian case are preserved for infinite waveguide case in polar coordinates. But one should consider each case individually, because form of fundamental solution is different for each coordinate system (for example, exponents in cartesian coordinates, Bessel and Hankel functions in polar).

2.2.2 Finite structures

Every finite structure can be considered as series of a 'unit' symmetrical periodicity cell (see Fig 1.2). In order to find eigenfrequencies interfacial conditions should be stated:

$$\begin{aligned} &u_1(\lambda) = u_2(\lambda) \\ &u'_1(\lambda) = \alpha\beta u'_2(\lambda) \\ &u_2((1+\gamma)\lambda) = u_3((1+\gamma)\lambda) \\ &\alpha\beta u'_2((1+\gamma)\lambda) = u'_3((1+\gamma)\lambda) \end{aligned} \tag{2.32}$$

And two types of boundary conditions (see App.A for Hamilton's principle explanation):

$$\begin{aligned} &u_1(\lambda/2) = 0 \\ &u_3((3/2+\gamma)\lambda) = 0 \end{aligned} \tag{2.33}$$

$$\begin{aligned} &-u'_1(\lambda/2) = 0 \\ &u'_3((3/2+\gamma)\lambda) = 0 \end{aligned} \tag{2.34}$$

Equations Eq.2.32-Eq.2.33 defines eigenfrequency problem with "fixed" ends or A-type border conditions, equations Eq.2.32 and Eq.2.34 defines problem with "free" ends or B-type border conditions (existence of two such types of conditions were predicted by J. Mead in [2]). Roots, obviously, can be found only numerically, since there are no inverse of the Bessel function exists. Eigenfrequencies in both problems converges to gap band borders with increasing of the frequency:

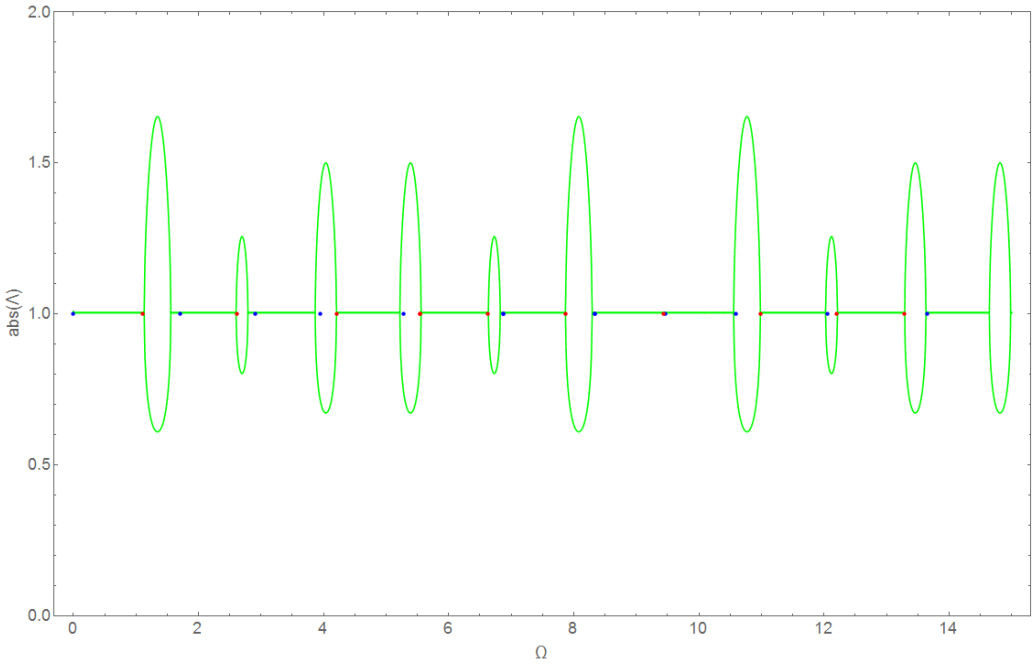

Figure 2.8: Eigenfrequency of single symmetric periodicity cells (red – eigenfrequencies of "fixed" problem, blue – "free")

As in axial case, all eigenfrequencies of more than one periodicity cell appears in pass bands and all eigenfrequencies from a lesser structure exists in a bigger:

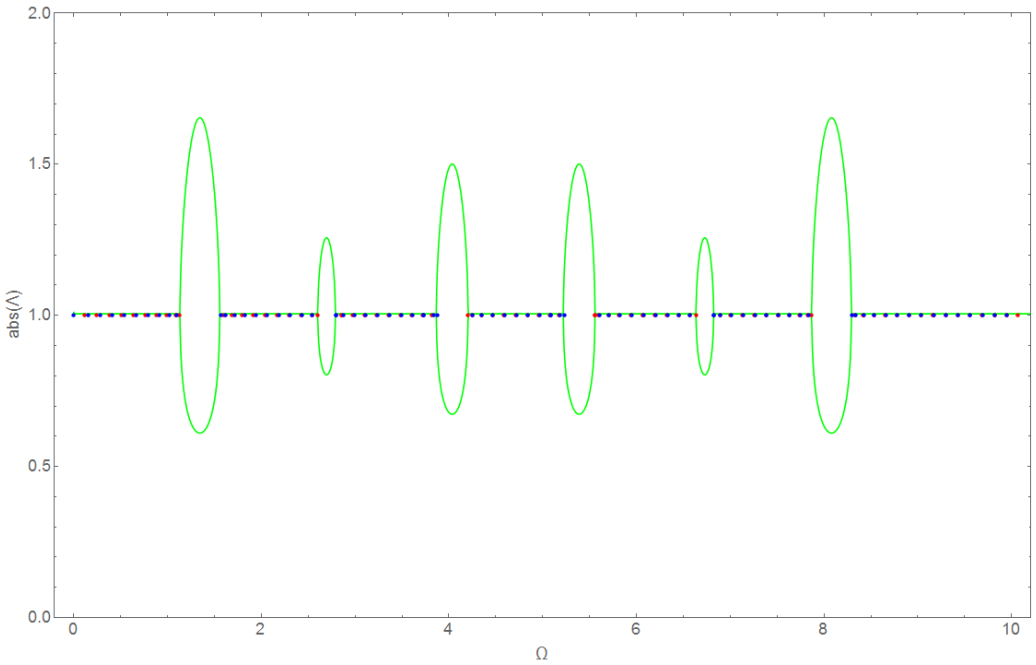

Figure 2.9: Eigenfrequency of structure with 10 symmetrical periodicity cells

In this chapter main patterns which are typical for periodical structure are shown. Behavior of eigenfrequencies of finite structure has very common pattern. Eigenfrequencies of axial and flexural rod vibrations, cylindrical shell single symmetrical cell also covers gap bands borders [7, 8]. Eigenfrequencies of several periodicity cells appears in pass bands in all cases. Also, shown techniques (Floquet theorem, boundary integrals method) that will be used in the next chapters. As seen, main patterns valid for cartesian coordinate system preserves in polar coordinates, but some adjustments required in order to show exact correspondence between these coordinate systems. Since membrane equation is closely related to a thin plate equation it gives reason to say that Floquet theory is working for circular thin plate equation, which will be used for modelling in second part of this work. Moreover, it gives reason to say that Floquet theory is coordinate independent and can be, with some adjustment,used for any coordinate system.

Chapter 3

Bernoulli-Euler curved beam model

In this chapter a simplified model of a torque vibration isolator is considered. Methods from previous chapter (Floquet theorem, boundary integrals method) have broad range of applicability. In this chapter all these methods are used for more complicated case of system of differential equations. This chapter has theoretical and practical goals. Practical goal is to build first model of torque vibration isolator in the form of a system of a differential equations. Theoretical goal is to show the difference between the picture of Floquet zones of a single differential equation and a system of differential equations. In order to achieve that, methods, considered in Ch.2 are expanded and full range of tools for system of differential equations is obtained.

Torque vibration isolator has following periodicity cell with two different parts illustrated on the Fig. 3.1

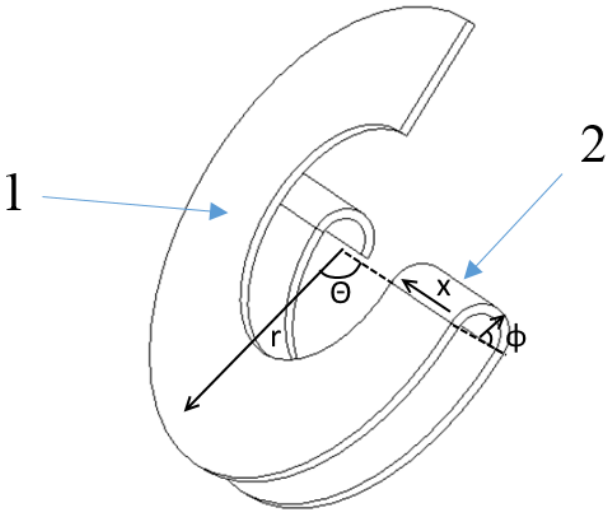

Figure 3.1: Vibration torque part

Part one is the segment of a circular plate, which is similar to a membrane considered in Ch.2 with a local polar coordinates (r, Θ) and part two is the segment of a thin cylindrical shell with local cartesian coordinate x and local polar angle ϕ. Each of these elements are more stiffer in transverse direction r and x than in longitudinal Θ and ϕ. Thus,as first approximation, the curved Bernoulli-Euler beam model can be used, which excludes deformation of the plate segment in r-coordinate and of the shell segment in x-coordinate.

As 'proof-of-concept' a curved beam with circular cross-section will be considered, because its consideration is obviously simpler. A curved beam has only one local coordinate s which is shown on Fig.3.2. Coordinate s is the natural parameter of a curve that connects geometrical center of each cross-section:

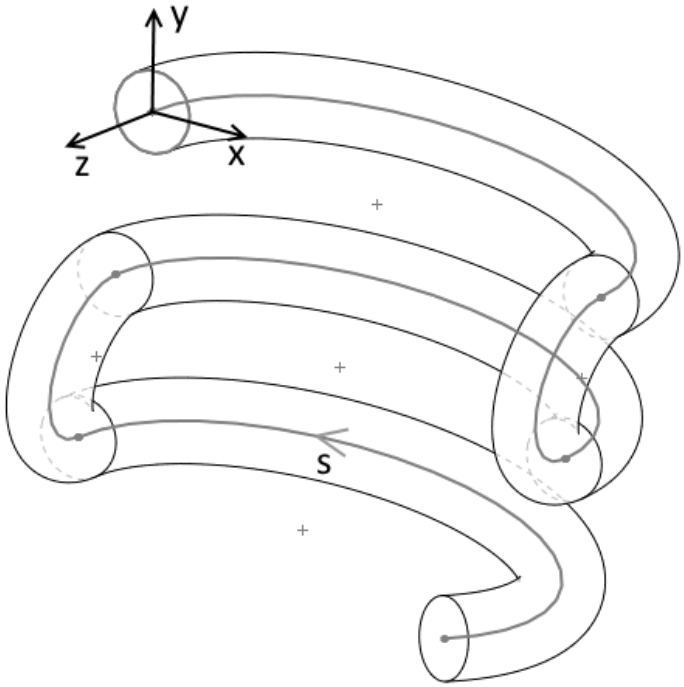

Figure 3.2: First model scheme

For each segment of the structure, shown on Fig.3.2 in-plane and out-plane vibrations can be considered separately.

3.1 Equations of motion

3.1.1 In-plane vibrations

With coordinate system shown on Fig.3.10 equations of motion of flat ring in-plane vibrations have the form [14]:

$$\begin{array}{l} \rho A\frac{\partial^2 u}{\partial t^2} = \frac{\partial Q_x}{\partial s} + \frac{1}{R}N_z + p_u - \frac{\partial p_\beta}{\partial s} \\ \rho A\frac{\partial^2 w}{\partial t^2} = \frac{\partial N_z}{\partial s} - \frac{1}{R}Q_x + p_w + \frac{1}{R}p_\beta \end{array} \tag{3.1}$$

,where u - x-axis displacement, w - z-axis displacement, β - rotation with respect to y axis, Q_i, N_i - components of force vector, M_i, T_i-components of moment vector, R is the radius of curvature. Generalized forces and rotation with Bernoulli-Euler assumptions have form:

$$\begin{array}{l} \frac{M_y}{EI_y} = \frac{\partial \beta}{\partial s}\,, Q_x = -\frac{\partial M_y}{\partial s} \\ \frac{N_z}{EA} = \frac{\partial w}{\partial s} - \frac{1}{R}u\,, \beta = \frac{\partial u}{\partial s} + \frac{1}{R}w \end{array} \tag{3.2}$$

For brevity no external loading considered, i.e. $p_u = p_w = p_\beta \equiv 0$

Time and space dependence for both in-plane and out-plane vibration has the form:

$$\{u(\bar{s},t), v(\bar{s},t), w(\bar{s},t), \gamma(\bar{s},t)\}^T = \{\bar{U}, \bar{V}, \bar{W}, \Gamma\}^T exp(k_{\dim}\bar{s} - i\omega t) \tag{3.3}$$

Following dimensionless parameters used:

$$\Omega = \frac{\omega d}{c}, k = k_{\dim} d, s = \frac{\bar{s}}{d}, U = \frac{\bar{U}}{d}, V = \frac{\bar{V}}{d}, W = \frac{\bar{W}}{d}, \varepsilon = \frac{d}{R} \tag{3.4}$$

With time and space dependence Eq.3.3 and dimensionless parameters Eq.3.4substituted into the system Eq.3.1-Eq.3.2 following system is obtained:

$$\begin{array}{l} W\left(16\mathrm{k}\varepsilon-\mathrm{k}^3\varepsilon\right)+U\left(-\mathrm{k}^4-16\varepsilon^2+16\Omega^2\right)=0 \\ U\left(-16\mathrm{k}\varepsilon+\mathrm{k}^3\varepsilon\right)+W\left(16\mathrm{k}^2+\mathrm{k}^2\varepsilon^2+16\Omega^2\right)=0 \end{array} \tag{3.5}$$

Determinant of system of algebraical linear equations Eq.3.5 gives 6th order polynomial in k, which is called dispersion relation:

$$k^6+k^4\Omega^2+2k^4\varepsilon^2-16k^2\Omega^2+k^2\varepsilon^4-k^2\Omega^2\varepsilon^2-16\Omega^4+16\Omega^2\varepsilon^2 \tag{3.6}$$

When it is solved with respect to k it gives 6 wavenumbers $k_i^{(in)}$:

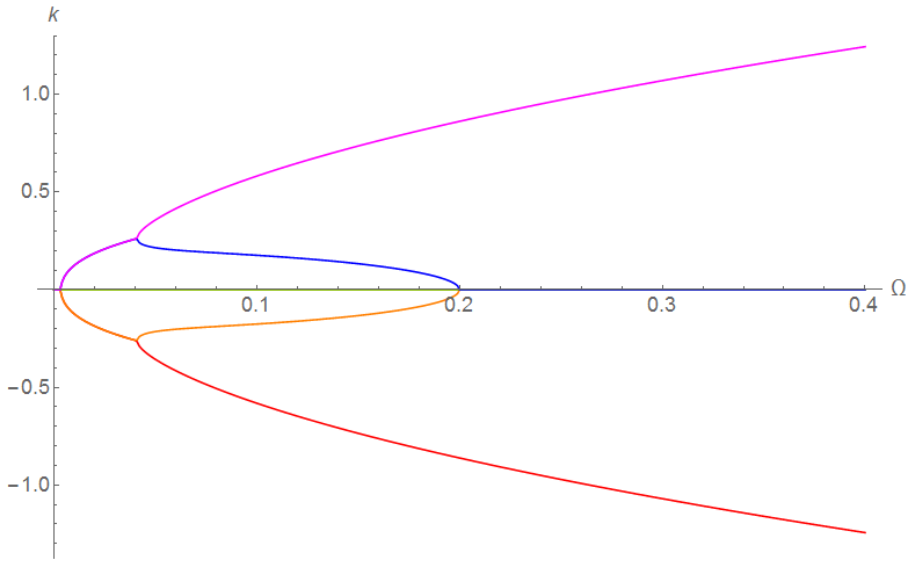

Figure 3.3: Wave numbers $k^{(in)}$, real parts

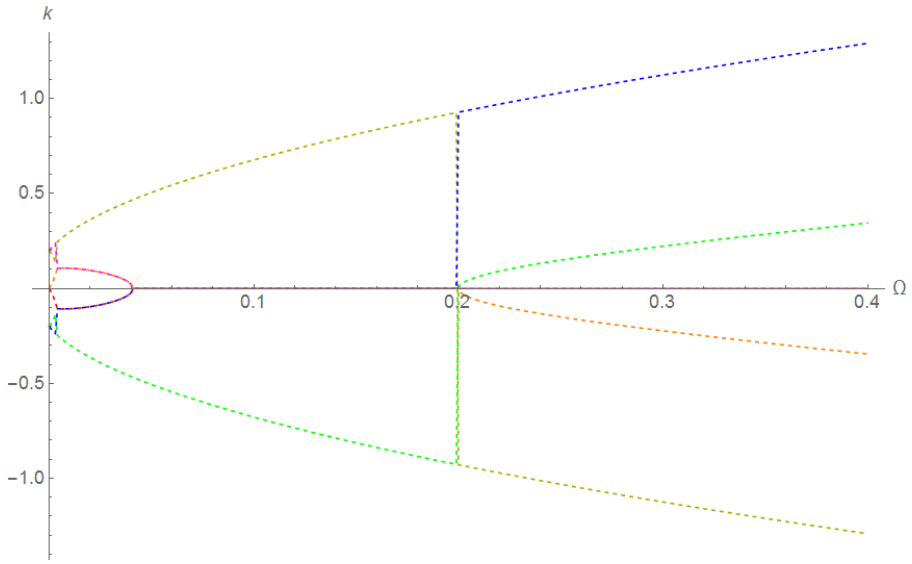

Figure 3.4: Wave numbers $k^{(in)}$, imaginary parts

For applications it is of interest to consider low-frequency range, therefore it shows pictures, that is characteristic only for Bernoulli-Euler curved beam:

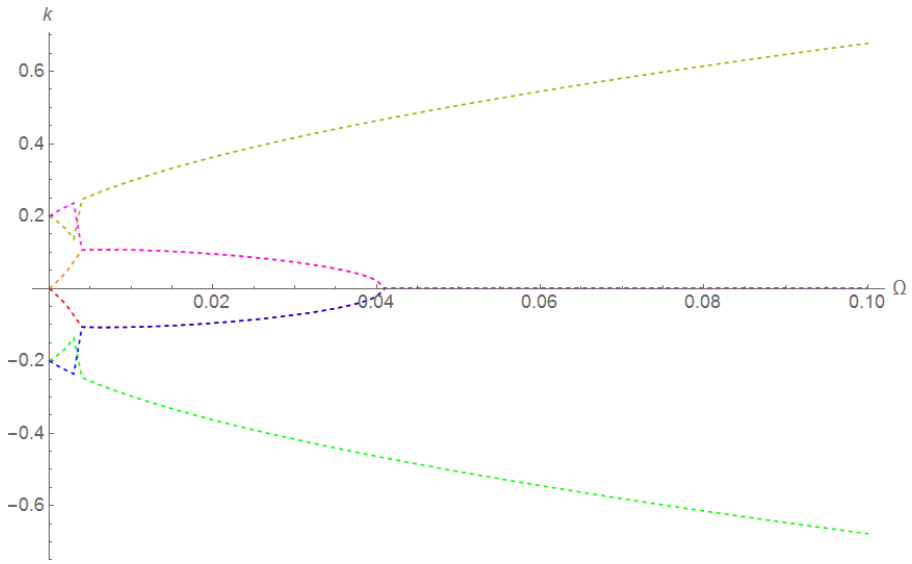

Figure 3.5: Wave numbers $k^{(in)}$, imaginary parts

Different forms of wave number k_i represents different form of waves. At the given frequency Ω, value $k(\Omega)$ can be pure real, pure imaginary and complex number. Since space dependence $\exp(k\,s)$ considered, pure imaginary $k(\Omega)$ represents propagating wave (wave that does not change its absolute value when s is changing). Main theorem of algebra state that if ik_{im} is the root of dispersion relation, then $-ik_{im}$ also the root. Root ik_{im} defines wave propagating from left to right (with time dependence $\exp(-i\omega t)$) and root $-ik_{im}$ defines wave propagating from right to left. Pure real value k_{re} represents evanescent waves (waves that exponentially decreasing from left to right or from right to left):

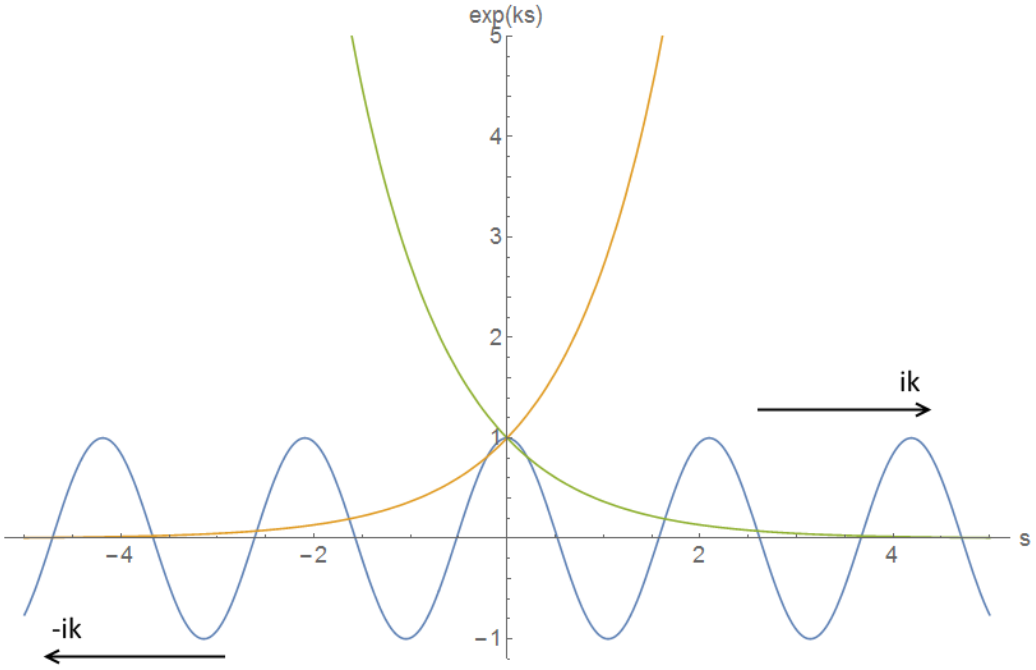

Figure 3.6: Different form of waves: pure imaginary ik_{im} (blue), pure real $k_{re} > 0$ (orange), pure real $k_{re} < 0$ (green)

Complex value represents wave $k_{comp} = k_{comp}^{(re)} + ik_{comp}^{(im)}$, propagating from left to right or from right to left (depends on a sign of imaginary part $k_{comp}^{(im)}$) modulated by $\exp(k_{comp}^{(re)}s)$,i.e. oscillating between two curves $\exp(k_{comp}^{(re)}s)$ and $-\exp(k_{comp}^{(re)}s)$ (shown dashed on the following figure) :

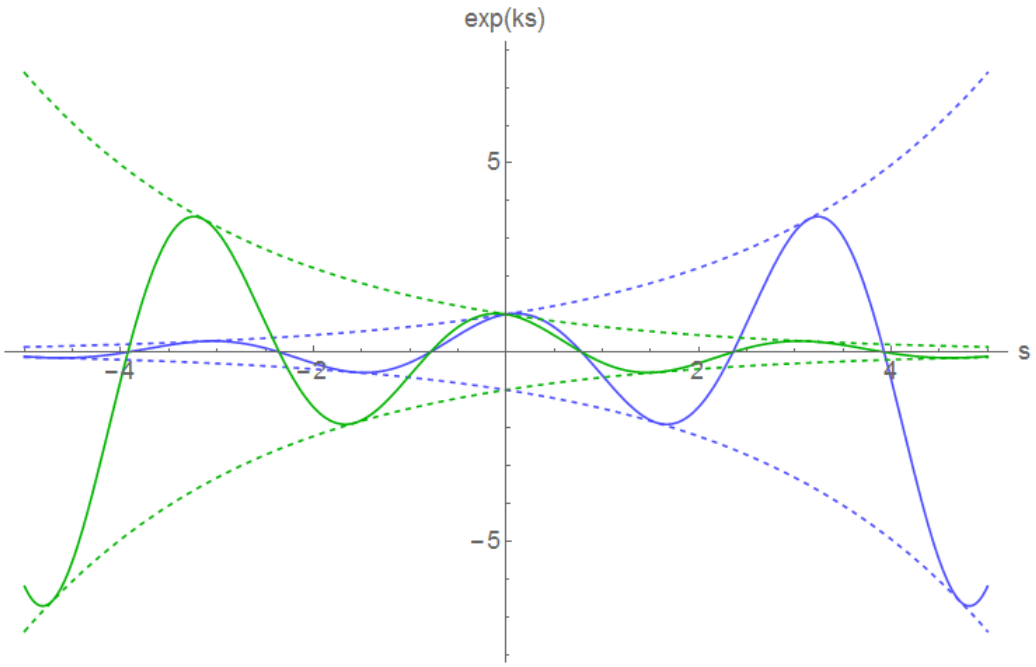

Figure 3.7: Different form of waves $k_{comp} = k_{comp}^{(re)} + ik_{comp}^{(im)}$: $k_{comp}^{(re)} > 0$ (blue), $k_{comp}^{(re)} < 0$ (green)

It is also convenient to introduce modal coefficient $m_w = \frac{W}{U}$, which is found from equations Eq.3.5 for each wave number individually. In that case $m_u = \frac{U}{U} = 1$. Also, modal coefficients for forces, moments and rotation introduced as:

$$\begin{aligned} m_\beta &= (k\, m_u + \varepsilon\, m_w) \\ m_{My} &= (k\, m_\beta) \\ m_{Nz} &= 16\,(k\, m_w - \varepsilon\, m_u) \\ m_{Qx} &= -k\, m_{My} \end{aligned} \tag{3.7}$$

3.1.2 Out-plane vibrations

Equations of motion of flat ring in-plane vibrations have the form:

$$\begin{aligned} \rho I_p \frac{\partial^2 \gamma}{\partial t^2} &= \frac{\partial T_z}{\partial s} - \frac{1}{R} M_x + p_\gamma \\ \rho A \frac{\partial^2 v}{\partial t^2} &= \frac{\partial Q_y}{\partial s} + p_v + \frac{\partial p_\alpha}{\partial s} \end{aligned} \tag{3.8}$$

With generalized forces and rotation with Bernoulli-Euler assumptions in form:

$$\begin{aligned} \frac{M_x}{EI_x} &= \frac{\partial \alpha}{\partial s} + \frac{1}{R}\gamma\,, \frac{T_z}{GI_p} = \frac{\partial \gamma}{\partial s} - \frac{1}{R}\alpha \\ Q_y &= \frac{\partial M_x}{\partial s} + \frac{1}{R} T_z\,, \alpha = -\frac{\partial v}{\partial s} \end{aligned} \tag{3.9}$$

Where, v - y-axis displacement, α - rotation with respect to x-axis, γ - rotation with respect to z-axis. With time and space dependence Eq.3.3 and dimensionless parameters Eq.3.4substituted into the system Eq.3.8-Eq.3.9 following system is obtained:

$$\begin{aligned} \Gamma\left(\frac{k^2}{\nu+1} + 2\Omega^2 - \varepsilon^2\right) + V\left(\frac{k^2\varepsilon}{\nu+1} + k^2\varepsilon\right) &= 0 \\ \Gamma\left(\frac{k^2\varepsilon}{\nu+1} + k^2\varepsilon\right) + V\left(-k^4 + \frac{k^2\varepsilon^2}{\nu+1} + 16\Omega^2\right) &= 0 \end{aligned} \tag{3.10}$$

Determinant of the system Eq.3.10:

$$-k^6 - 2k^4\nu\Omega^2 - 2k^4\Omega^2 - 2k^4\varepsilon^2 + 16k^2\Omega^2 - k^2\varepsilon^4 + 2k^2\Omega^2\varepsilon^2 + 32\nu\Omega^4 + 32\Omega^4 - 16\nu\Omega^2\varepsilon^2 - 16\Omega^2\varepsilon^2 \tag{3.11}$$

Also gives 6 wavenumbers $k_i^{(out)}$:

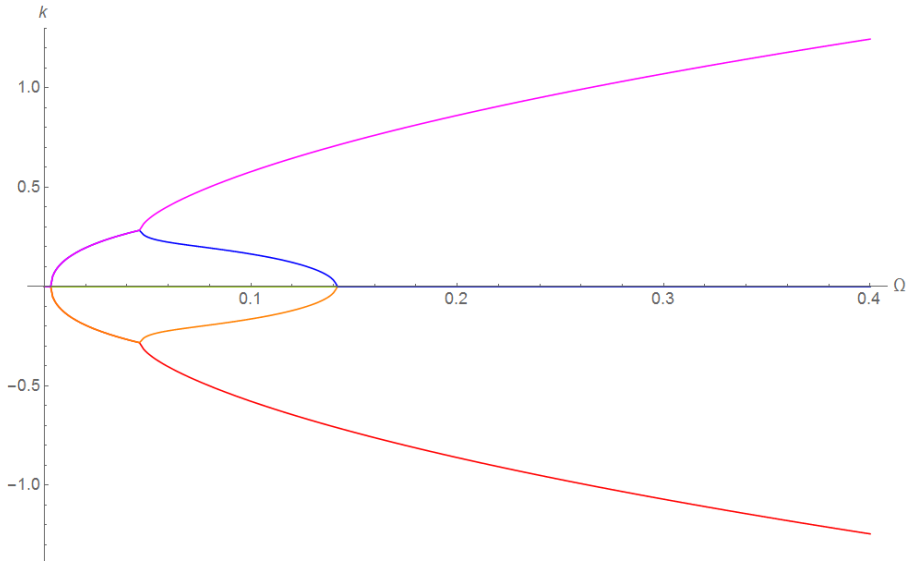

Figure 3.8: Wave numbers $k^{(out)}$, real parts

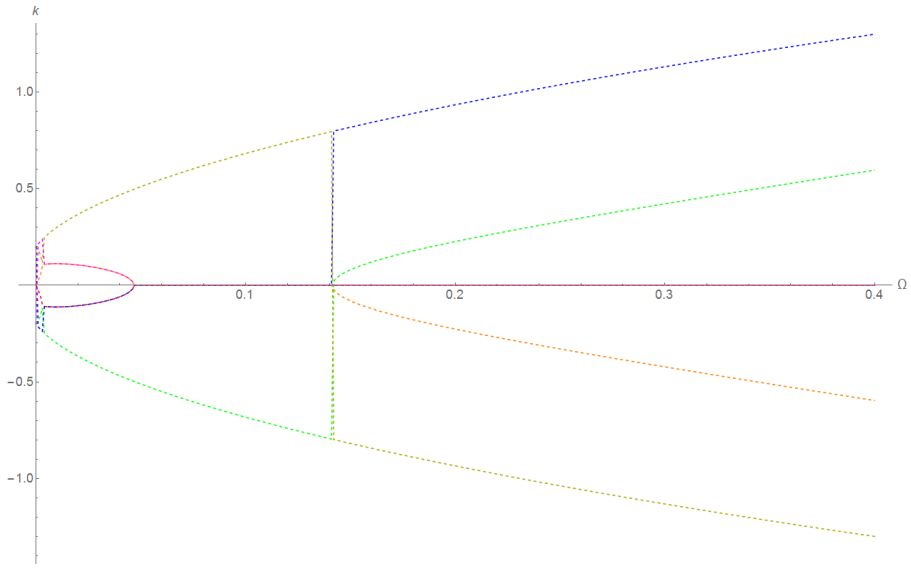

Figure 3.9: Wave numbers $k^{(out)}$, imaginary parts

Modal coefficients in this case have form:

$$\begin{array}{ll} m_\gamma = 1 & m_v = \frac{V}{\Gamma} \\ m_\alpha = -k m_v & m_{My} = (k\, m_\alpha + \varepsilon m_\gamma) \\ m_{Tz} = \frac{1}{1+\nu}\,(k\, m_\gamma - \varepsilon\, m_\alpha) & m_{Qy} = k\, m_{Mx} + \varepsilon m_{Tz} \end{array} \tag{3.12}$$

3.2 Boundary integrals method

Definition of Green's matrix for a system of a differential equation is the same as for Green's function for a single equation, but in case of n equations with m variable functions n load cases should be considered. In each case one load is represented by delta-function whereas other are zero. Therefore, Green's matrix has dimensions $n \times m$.

Since in boundary integrals method Green's matrix for infinite structure considered, Green's matrix should satisfy radiation and decay conditions at the infinity [12]. Therefore, not all wavenumbers can be considered. Detailed explanation of principle of choice and all necessary references contained in [14]. Among six roots of both dispersion relations we choose one complex with negative real part ($Re(k) < 0$) and two purely imaginary roots with $c_{group} = \frac{dk_{din}}{d\omega} > 0$ for each in-plane and out-plane equations.

For Green's matrix derivation bi-orthogonality condition will be used. It can be derived from reciprocity theorem, which is well known for most commonly used linear differential equations and for elastic helical spring is described in [13]. Derivation of all bi-orthogonality conditions used here can be found in [9].

3.2.1 In-plane vibrations

Bi-orthogonality condition for this case has the form:

$$M_y^A(s)\beta^B(s) + N_z^A(s)w^B(s) - u^A(s)Q_x^B(s) = 0 \tag{3.13}$$

Or with modal coefficients introduced in Eq. 3.10:

$$m_{My}^{(i)}\, m_{\beta}^{(j)} + m_{Nz}^{(i)}\, m_{w}^{(j)} - m_{u}^{(i)}\, m_{Qx}^{(j)} = 0 \ (i \neq j) \tag{3.14}$$

Equations Eq.3.13-Eq.3.24 are called bi-orthogonality conditions for flat ring in-plane vibrations. And with reciprocity theorem they are widely used in Green's functions theory and for boundary integral equations derivation.

In in-plane ring vibrations case each string of Green's matrix represents solution for each of a loading case $p_i = \delta(s)$, $p_j = 0\,(i \neq j\ ;\ i,j \in \{u, w, \beta\})$

In order to find Green's matrix, property of force unit jump of Green's function also used. Three load cases considered: load case 1 $N_z(0) = -\frac{1}{2}sign(s)$ (it represents case $p_w = \delta(s)$), load case 2 $M_y(0) = -\frac{1}{2}sign(s)$ $(p_\beta = \delta(s))$ and load case 3 $Q_x(0) = -\frac{1}{2}sign(s)$ $(p_u = \delta(s))$. With that loading cases introduced it is convenient to split Forces/Moments and displacements into two groups:

$$\begin{array}{l} \{w(s), \beta(s), Q_x(s)\} \\ \{u(s), N_z(s), M_y(s)\} \end{array} \tag{3.15}$$

If functions of first group are even, then functions of second group are odd and vice versa. Since Heaviside theta-function is odd function, only continuity of functions should be considered. Even functions have property of continuity at zero, and therefore, functions of second group are continuous.

Let us consider loading case 1. Significant part of Green's matrix has a following form:

$$\{u(s), N_z(s), M_y(s)\} = \sum_{i=1}^{3} \{m_u^{(i)}, m_{Nz}^{(i)}, m_{My}^{(i)}\}\Gamma_i^{(1)} \exp(k_i\, abs(s))sign(s) \tag{3.16}$$

Properties of Green's matrix have following form:

$$\begin{array}{l} u(0) = 0 \\ M_y(0) = 0 \\ N_z(0) = -\frac{1}{2}sign(s) \end{array} \tag{3.17}$$

Substituting 3.16 to 3.17 and multiplying each string to $m_{Qx}^{(j)}$, $m_{\beta}^{(j)}$, $m_{w}^{(j)}$ $(j = 1, 2, 3)$ respectively:

$$\begin{aligned}
&\sum_{i=1}^{3} \Gamma_i^{(1)} m_u^{(i)} m_{Qx}^{(j)} = 0 \\
&\sum_{i=1}^{3} \Gamma_i^{(1)} m_{My}^{(i)} m_\beta^{(j)} = 0 \\
&\sum_{i=1}^{3} \Gamma_i^{(1)} m_N z^{(i)} m_w^{(j)} = -\tfrac{1}{2}
\end{aligned} \tag{3.18}$$

Summing all equations in 3.18:

$$\sum_{i=1}^{3} \Gamma_i^{(1)} (m_u^{(i)}\, m_{Qx}^{(j)} + m_{My}^{(i)}\, m_\beta^{(j)} + m_{Nz}^{(i)}\, m_w^{(j)}) = -\frac{1}{2} \tag{3.19}$$

Expression in brackets is exactly bi-orthogonal condition 3.24 and it is not zero only when $i = j$. Thus one can obtain explicit form of each coefficient $\Gamma_i^{(1)}$.

In same way all Green's matrix coefficient entries can be found as:

$$\begin{aligned}
\Gamma(in)_i^{(1)} &= -\tfrac{1}{2} \frac{m_w^{(i)}}{m_{My}^{(i)}\, m_\beta^{(i)} + mNz_i\, m_w^{(i)} - m_u^{(i)}\, m_{Qx}^{(i)}} \\
\Gamma(in)_i^{(2)} &= -\tfrac{1}{2} \frac{m_\beta^{(i)}}{m_{My}^{(i)}\, m_\beta^{(i)} + mNz_i\, m_w^{(i)} - m_u^{(i)}\, m_{Qx}^{(i)}} \\
\Gamma(in)_i^{(3)} &= \tfrac{1}{2} \frac{m_u^{(i)}}{m_{My}^{(i)}\, m\beta_i + mNz_i\, m_w^{(i)} - m_u^{(i)}\, m_{Qx}^{(i)}}
\end{aligned} \tag{3.20}$$

After coefficients found green matrix formed as (on example of loading case 1):

$$\begin{aligned}
&G_1^{in}(s, s_0) = \{u^{(n)}(s), w^{(n)}(s), \beta^{(n)}(s), Q_x^{(n)}(s), N_z^{(n)}(s), M_y^{(n)}(s)\} = \\
&\sum_{i=1}^{3} \{sign(s)\, m_u^{(i)}, m_w^{(i)}, m_\beta^{(i)}, m_{Qx}^{(i)}, sign(s)\, mNz_i, sign(s)\, m_{My}^{(i)}\} \Gamma(in)_i^{(1)} \exp(k_i^{in}\, abs(s - s_0))
\end{aligned} \tag{3.21}$$

After Green's matrix found, one can obtain displacement, expressed in terms of Green's matrix (analogous to 2.13) in same way as it done in App.B. It can be written as ([13]):

$$\delta_{1n} w(s_0) + \delta_{2n} \beta(s_0) + \delta_{3n} u(s_0) = \left[G_n^{in}(s, s_0).\, \{Q_x(s), Nz(s), My(s), -u(s), -w(s), -\beta(s)\} \right]_{s=a}^{s=b} \tag{3.22}$$

,where δ_{ij} -Kronecker's delta and $\{\}.\{\}$ - dot product of two vectors. Equations Eq.**??** called boundary integrals for ring in-plane vibrations.

3.2.2 Out-plane vibrations

In same way, with three loading cases: load case 1 $Q_y(0) = -\frac{1}{2} sign(s)$ ($p_u = \delta(s)$), load case 2 $T_z(0) = -\frac{1}{2} sign(s)$ ($p_\gamma = \delta(s)$) and load case 3 $M_x(0) = -\frac{1}{2} sign(s)$ ($p_\alpha = \delta(s)$).

Two groups of functions:

$$\begin{aligned}
&\{v(s), \gamma(s), M_x(s)\} \\
&\{\alpha(s), T_z(s), Q_y(s)\}
\end{aligned} \tag{3.23}$$

And bi-orthogonality condition:

$$m_{Tz}^{(i)}\, m_\gamma^{(j)} + m_{Qy}^{(i)}\, m_v^{(j)} - m_\alpha^{(i)}\, m_{Mx}^{(j)} = 0 \ (i \neq j) \tag{3.24}$$

One can obtain Green's matrix coefficients in form:

$$\begin{aligned}\Gamma(out)_i^{(1)} &= -\frac{1}{2}\frac{m_v^{(i)}}{m_{Tz}^{(i)} m_\gamma^{(i)} + m_{Qy}^{(i)} m_v^{(i)} - m_\alpha^{(i)} m_{Mx}^{(i)}} \\ \Gamma(out)_i^{(2)} &= -\frac{1}{2}\frac{m_\gamma^{(i)}}{m_{Tz}^{(i)} m_\gamma^{(i)} + m_{Qy}^{(i)} m_v^{(i)} - m_\alpha^{(i)} m_{Mx}^{(i)}} \\ \Gamma(out)_i^{(3)} &= \frac{1}{2}\frac{m_\alpha^{(i)}}{m_{Tz}^{(i)} m_\gamma^{(i)} + m_{Qy}^{(i)} m_v^{(i)} - m_\alpha^{(i)} m_{Mx}^{(i)}}\end{aligned} \tag{3.25}$$

Green's matrix in form:

$$\begin{aligned}&G_1^{out}(s, s_0) = \{v^{(n)}(s), \alpha^{(n)}(s), \gamma^{(n)}(s), Q_y^{(n)}(s), M_z^{(n)}(s), T_z^{(n)}(s)\} = \\ &\sum_{i=1}^{3} \{m_v^{(i)}, sign(s)\, m_\alpha^{(i)}, m\gamma_i, sign(s)\, m_{Qy}^{(i)}, m_{Mx}^{(i)}, sign(s)\, m_{Tz}^{(i)}\} \Gamma(out)_i^{(1)} \exp(k_i^{out}\, abs(s - s_0))\end{aligned} \tag{3.26}$$

And boundary equations in form:

$$\delta_{1n} v(s_0) + \delta_{2n}\gamma(s_0) + \delta_{3n}\alpha(s_0) = \left[G_n^{out}(s, s_0).\, \{Q_y(s), Mx(s), Tz(s), -u(s), -\alpha(s), -\gamma(s)\}\right]_{s=a}^{s=b} \tag{3.27}$$

3.3 The benchmark periodic structure

In order to validate the theory and the Wolfram Mathematica codes, an auxiliary problem has been considered first.

3.3.1 Infinite periodic structure

With respect to natural coordinate s ring can be considered as periodic structure shown on the Fig.1.2. Similar problem was considered in [3] for a helical spring and flat ring, but it was considered within Timoshenko beam theory. In this work, as stated above Bernoulli-Euler theory considered.

Let us consider a auxiliary problem with parts of periodicity structure connected such that plane of in-plane vibrations of both parts are the same. Finally model can be represented as:

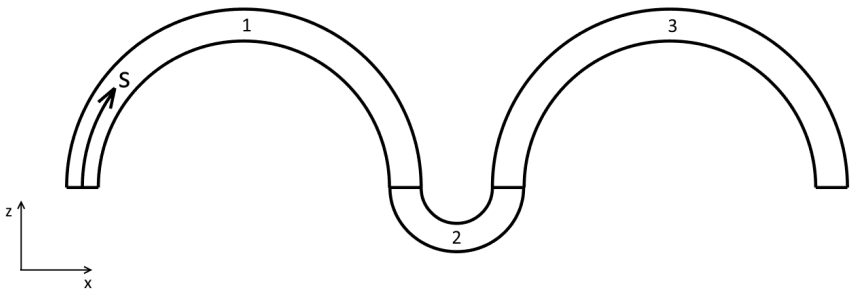

Figure 3.10: Auxiliary problem scheme

Each curved beam segment has the same material and same wire diameter, but different curvature radius. Additional dimensionless parameters introduced as:

$$\alpha = \frac{E_1}{E_2}; \gamma = \frac{l_2}{l_1};\ \sigma = \frac{c_2}{c_1}; \lambda = \frac{l_1}{d};\ \Omega_1 = \Omega;\ \Omega_2 = \frac{\Omega}{\sigma};\ \ \varepsilon_1 = \frac{d}{R_1};\ \varepsilon_2 = \frac{d}{R_2} \tag{3.28}$$

Hereafter following dimensionless parameters set is considered unless it is stated otherwise:

$$\alpha = 1; \gamma = 0.5;\ \sigma = 1; \lambda = 5;\ \varepsilon_1 = 0.2;\ \varepsilon_2 = 0.02 \tag{3.29}$$

As in the case of axial and flexural beam vibrations Floquet theory can be used. Following notation used:

$$\begin{aligned} &disp_i(s) = \{w_i(s), \beta_i(s), u_i(s), v_i(s), \gamma_i(s), \alpha_i(s)\} \\ &force_i(s) = \tfrac{1}{E_i I_x^{(i)}}\{Q_x^{(i)}(s), N_z^{(i)}(s), M_y^{(i)}(s), Q_y^{(i)}(s), M_x^{(i)}(s), T_z^{(i)}(s)\} \end{aligned} \tag{3.30}$$

Let us consider three subsequent parts of ring. For each part of ring we define two set of three boundary integrals in form Eq.3.29 and Eq.3.35 (totally, 6*6=36 equations) and additionally interfacial conditions (4*6=24 equations):

$$\begin{aligned} &w_1(1) = w_2(1)\ ; \beta_1(1) = \beta_2(1)\ ; u_1(1) = u_2(1) \\ &\gamma_1(1) = \gamma_2(1)\ ; v_1(1) = v_2(1)\ ; \alpha_1(1) = \alpha_2(1) \\ &N_z^{(1)}(1) = \alpha_{par}\, N_z^{(2)}(1)\ ; M_y^{(1)}(1) = \alpha_{par}\, M_y^{(2)}(1)\ ; Q_x^{(1)}(1) = \alpha_{par}\, Q_x^{(2)}(1) \\ &T_z^{(1)}(1) = \alpha_{par}\, T_z^{(2)}(1)\ ; Q_y^{(1)}(1) = \alpha_{par}\, Q_y^{(2)}(1)\ ; M_x^{(1)}(1) = \alpha_{par}\, M_x^{(2)}(1) \\ &w_2(1+\gamma_{par}) = w_3(1+\gamma_{par})\ ; \beta_2(1+\gamma_{par}) = \beta_3(1+\gamma_{par})\ ; u_2(1+\gamma_{par}) = u_3(1+\gamma_{par}) \\ &\gamma_2(1+\gamma_{par}) = \gamma_3(1+\gamma_{par})\ ; v_2(1+\gamma_{par}) = v_3(1+\gamma_{par})\ ; \alpha_2(1+\gamma_{par}) = \alpha_3(1+\gamma_{par}) \\ &N_z^{(2)}(1+\gamma_{par}) = \alpha_{par}\, N_z^{(3)}(1+\gamma_{par})\ ; M_y^{(2)}(1+\gamma_{par}) = \alpha_{par}\, M_y^{(3)}(1+\gamma_{par}) \\ &Q_x^{(2)}(1+\gamma_{par}) = \alpha_{par}\, Q_x^{(3)}(1+\gamma_{par}) \\ &T_z^{(2)}(1+\gamma_{par}) = \alpha_{par}\, T_z^{(3)}(1+\gamma_{par})\ ; Q_y^{(2)}(1+\gamma_{par}) = \alpha_{par}\, Q_y^{(3)}(1+\gamma_{par}) \\ &M_x^{(2)}(1+\gamma_{par}) = \alpha_{par}\, M_x^{(3)}(1+\gamma_{par}) \end{aligned} \tag{3.31a}$$

Or in vector form:

$$\begin{aligned} &disp_1(1) = disp_2(1) \\ &force_1(1) = \alpha\, force_2(1) \\ &disp_2(1+\gamma) = disp_3(1+\gamma) \\ &\alpha force_2(1+\gamma) = force_3(1+\gamma) \end{aligned} \tag{3.31b}$$

And Floquet periodicity conditions (2*6=12 equations):

$$\begin{aligned} &u_1(0) = \Lambda\, u_3(1+\gamma);\quad v_1(0) = \Lambda\, u_3(1+\gamma);\quad w_1(0) = \Lambda\, u_3(1+\gamma) \\ &\alpha_1(0) = \Lambda\, \alpha_3(1+\gamma);\quad \beta_1(0) = \Lambda\, \beta_3(1+\gamma);\quad \gamma_1(0) = \Lambda\, \gamma_3(1+\gamma) \\ &M_x^{(1)}(0) = \Lambda\, M_x^{(3)}(1+\gamma);\quad M_y^{(1)}(0) = \Lambda\, M_y^{(3)}(1+\gamma);\quad T_z^{(1)}(0) = \Lambda\, T_z^{(3)}(1+\gamma) \\ &Q_x^{(1)}(0) = \Lambda\, Q_x^{(3)}(1+\gamma);\quad Q_y^{(1)}(0) = \Lambda\, Q_y^{(3)}(1+\gamma);\quad N_z^{(1)}(0) = \Lambda\, N_z^{(3)}(1+\gamma) \end{aligned} \tag{3.32a}$$

Or in vector form:

$$\begin{aligned} &disp_1(0) = \Lambda\, disp_3(1+\gamma) \\ &force_1(0) = \Lambda\, force_3(1+\gamma) \end{aligned} \tag{3.32b}$$

Boundary integrals with conditions Eq.3.31a-Eq.3.32b defines homogenous system of algebraical equations with respect to unknown displacements and forces on borders of the ring parts. Let $D(\Lambda, \Omega)$ be the determinant of this system. $D(\Lambda, \Omega)$ is the twelfth order polynomial in Λ , which defines stop- and pass-bands. It should be empathized, that determinant $D(\Lambda, \Omega)$

factorizes in two sixth order polynomials in Λ : in- and out- plane vibrations part, i.e. $D(\Lambda,\Omega) = D^{in}(\Lambda,\Omega) * D^{out}(\Lambda,\Omega)$. Therefore these two parts can be considered independently.

It should be noted that both of determinants $D^{in}(\Lambda,\Omega)$ and $D^{out}(\Lambda,\Omega)$ can be written in form:

$$D^*(\Lambda,\Omega) = \Lambda^6 + a_5\Lambda^5 + a_4\Lambda^4 + a_3\Lambda^3 + a_2\Lambda^2 + a_1\Lambda + 1 \tag{3.33}$$

It has two properties: 1.By Vieta theorem, since free term of polynomial $D^*(\Lambda,\Omega)$ is 1, if Λ is a root of polynomial Eq.3.33, then Λ^{-1} is a root of polynomial too. 2. It has only even powers of Ω as coefficients a_i because no damping is considered.

For further consideration it is convenient to write D^{in} as $D^{w,u}$ with meaning of flexural-axial part of a Floquet determinant. Also D^{out} written as $D^{\gamma,v}$ with meaning of flexural-torsional part.

One can plot dependency Λ of Ω, for example from condition $D^{w,u}(\Lambda,\Omega) = 0$. Unlike the cases considered earlier in [8] there exists three pairs (with property $\Lambda_1 * \Lambda_2 = 1$) of branches of solutions $\Lambda_i(\Omega)$: one pair of exponentially increasing and decreasing branches (this couple is not shown below, because this couple has significantly higher (and lower) magnitude than other two branches) and two pair of branches that defines stop- and pass-bands, it preserves for both determinants $D^{w,u}$ and $D^{\gamma,v}$. Below dependence $D^{w,u}(\Lambda,\Omega) = 0$ is plotted :

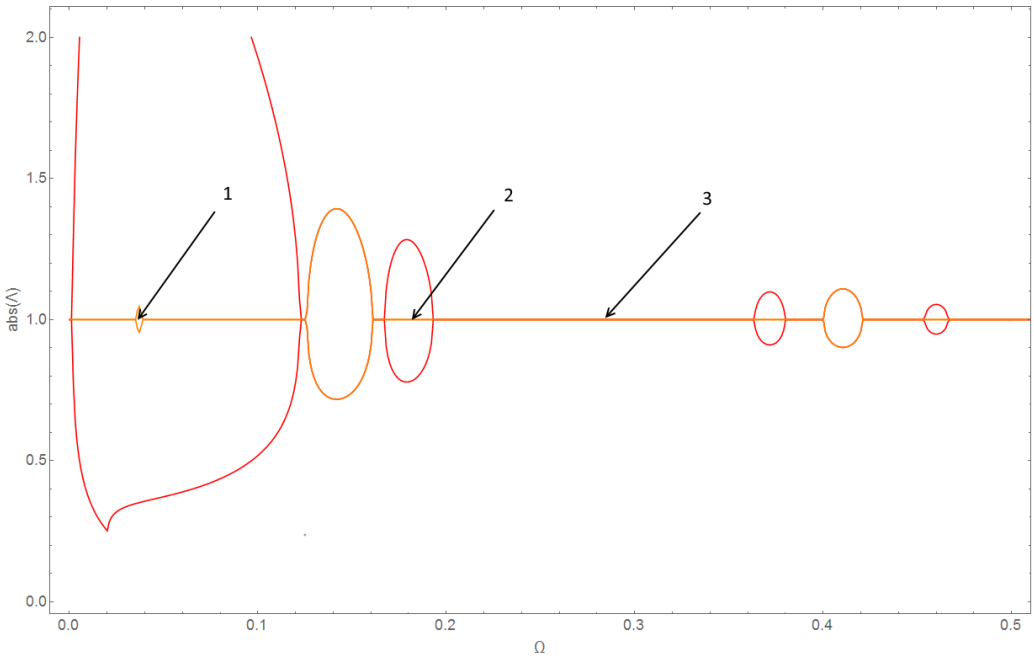

Figure 3.11: Floquet zones for $D^{w,u}(\Lambda,\Omega)$ and different kinds of zones marked with numbers

One can distinct “real” stop band (marked as 1), where wave propagation fully blocked,its location is defined by intersection of stop-bands of two branches (overlapping of an orange stop band and a red stop band on the Fig.3.11).In zone 1 only exponential increasing-decreasing standing waves are presented. "Partial"gap band (marked as 2) its location defined by overlapping pass band and stop band of different branches (overlapping of a red stop band and an orange pass band and vice versa). In zone 2 appears one propagating wave. And pass band (marked as 3) its location defined as overlapping of two pass bands of different branches (an orange pass band and a red pass band) in zone 3 two propagating waves are presented. All three zones contains one pair of standing exponential increasing-decreasing standing waves, which is described above and not shown on the picture.

Dependence $D^{out}(\Lambda,\Omega) = 0$ also have same form:

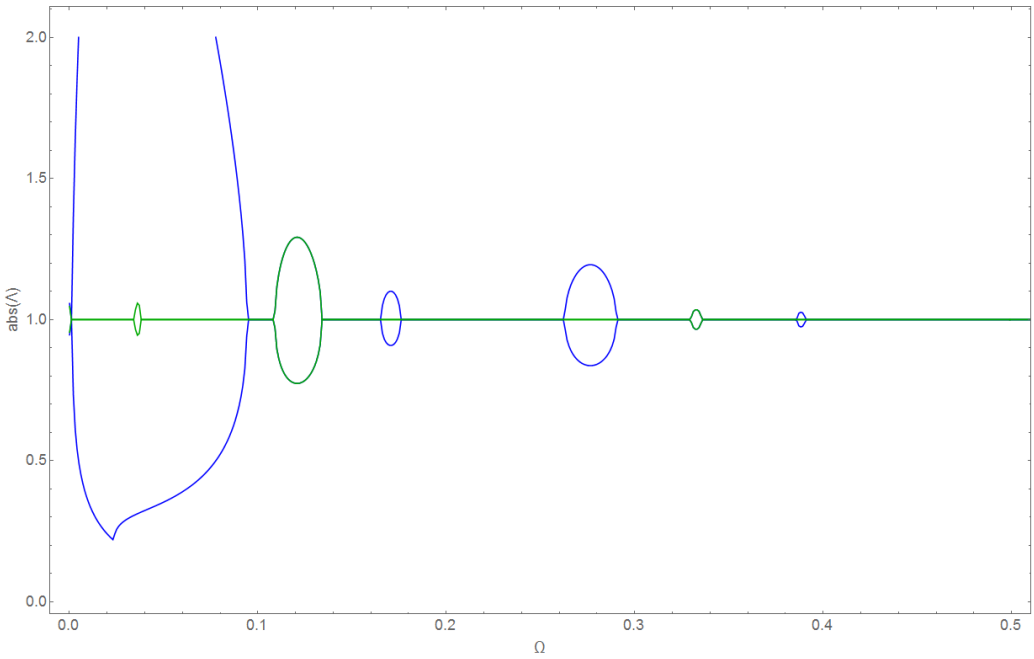

Figure 3.12: Floquet zones for $D^{\gamma,v}(\Lambda,\Omega)$

Since model considered as whole, both pictures for in-plane and out-plane vibrations should be considered simultaneously, but for visual reason they are separated. For comparison, both figures Fig.3.11 and Fig.3.12 shown in one plot:

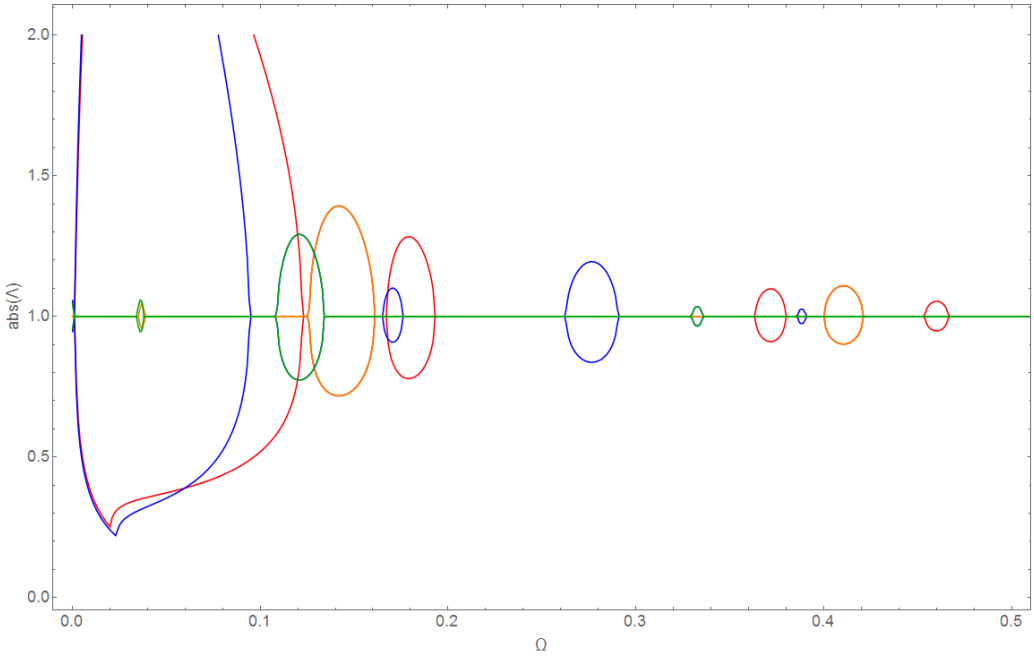

Figure 3.13: Floquet zones for $D(\Lambda,\Omega)$

As seen, there are zones, where all 6 branches have $\text{abs}(\Lambda) \neq 1$ and therefore full wave propagation is fully blocked. Presence of this kind of stop bands is proved theoretically and shown experimentally in [3] for flat ring and helical spring in frame of Timoshenko theory and both models, shown here and in article [3] are in agreement with each other.

3.3.2 Finite periodic structure

As in previous cases one can introduce concept of a symmetrical periodicity cell shown on the Fig.1.3

One can find eigenfrequencies of this structure. With properly selected symmetrical boundary conditions one can obtain boundary conditions on the gap band borders. In case of the ring in-plane vibrations it is two groups of functions Eq. 3.23 discussed earlier. A-type boundary conditions for one periodicity cell defined as [14]:

$$\begin{aligned}&\{w(\tfrac{1}{2}),\beta(\tfrac{1}{2}),Q_x(\tfrac{1}{2}),v(\tfrac{1}{2}),\gamma(\tfrac{1}{2}),M_x(\tfrac{1}{2})\}=0\\&\{w(\tfrac{3}{2}+\gamma_{par}),\beta(\tfrac{3}{2}+\gamma_{par}),Q_x(\tfrac{3}{2}+\gamma_{par}),v(\tfrac{3}{2}+\gamma_{par}),\gamma(\tfrac{3}{2}+\gamma_{par}),M_x(\tfrac{3}{2}+\gamma_{par})\}=0\end{aligned} \tag{3.34}$$

And B-type boundary conditions as:

$$\begin{aligned}&\{u(\tfrac{1}{2}),N_z(\tfrac{1}{2}),M_y(\tfrac{1}{2}),\alpha(\tfrac{1}{2}),Q_y(\tfrac{1}{2}),T_y(\tfrac{1}{2})\}=0\\&\{u(\tfrac{3}{2}+\gamma_{par}),N_z(\tfrac{3}{2}+\gamma_{par}),M_y(\tfrac{3}{2}+\gamma_{par}),\alpha(\tfrac{3}{2}+\gamma_{par}),Q_y(\tfrac{3}{2}+\gamma_{par}),T_z(\tfrac{3}{2}+\gamma_{par})\}=0\end{aligned} \tag{3.35}$$

Boundary integrals with interfacial conditions Eq.3.31a and boundary conditions Eq.3.34 or Eq.3.35 defines also homogenous system of linear algebraical equations with respect to unknown displacements and forces/moments at the ring parts borders. And by equaling determinant of this system to zero we can find eigenfrequencies. Eigenfrequencies of system Eq.3.34 and Eq.3.35 fully covers stop-band borders as in other cases considered in [8].

Determinant of the system Eq.3.31a, Eq.3.34 or Eq.3.31a, Eq.3.35 also can be factorized into two parts: in-plane and out-plane. And also both parts will be shown separately. In plane eigenfrequencies can be plotted as:

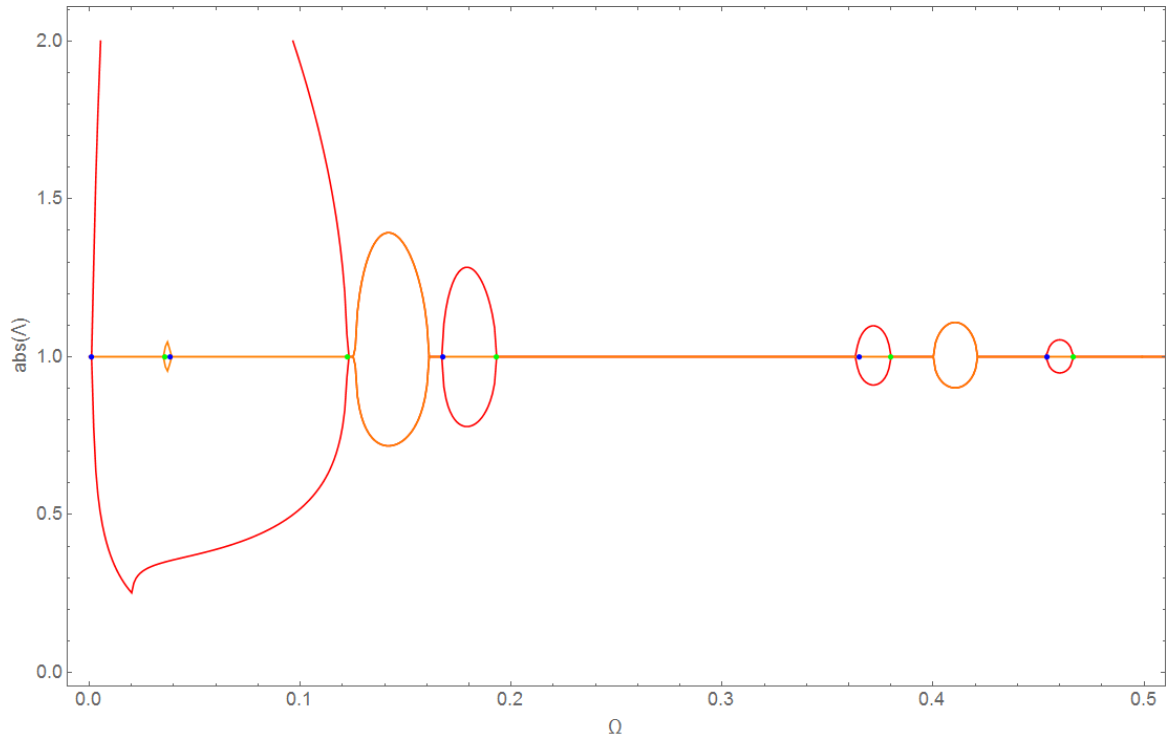

Figure 3.14: Eigenfrequencies of the single in-plane periodical cell: boundary conditions A (red) and boundary conditions B (green)

As seen property of eigenfrequencies of a single periodicity cell preserved. Eigenfrequency of a single periodicity cell appears only in gap bands borders and covers all borders of gap bands. If one considers out-plane periodicity cells, same property can be seen:

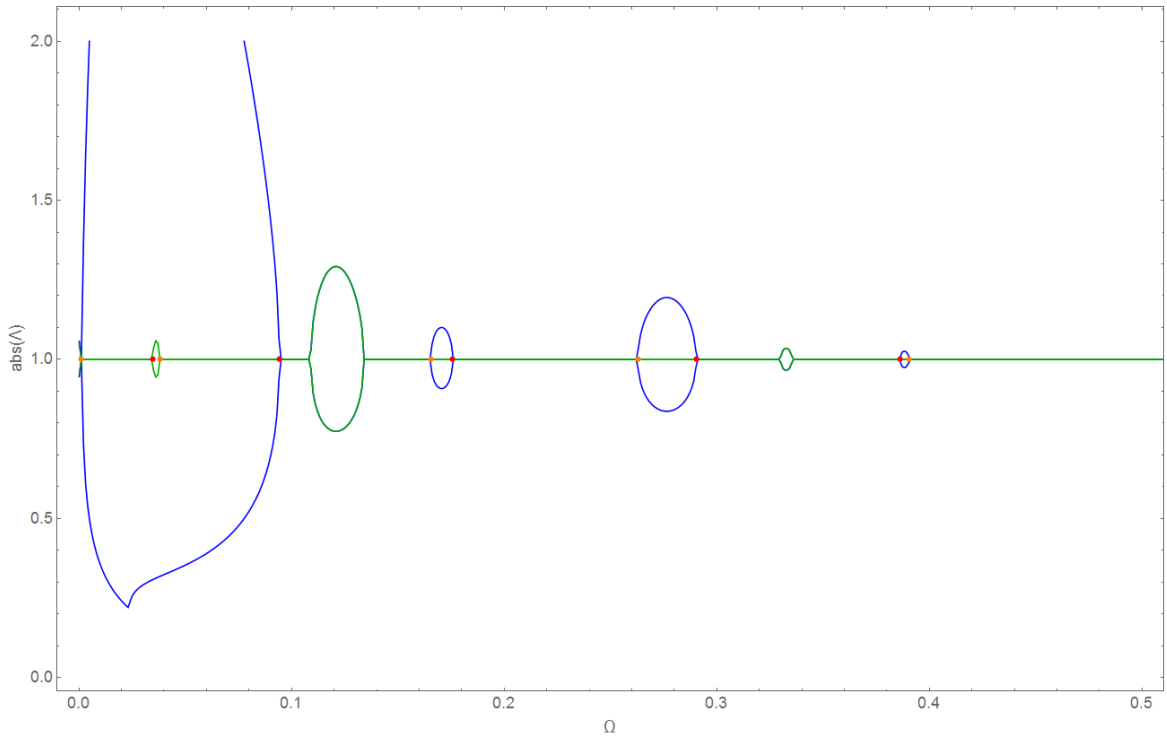

Figure 3.15: Eigenfrequency of single periodicity cell (out-plane part)

One can consider system with more periodicity cells and we see that new eigenfrequencies appears only in “pure” pass-bands:

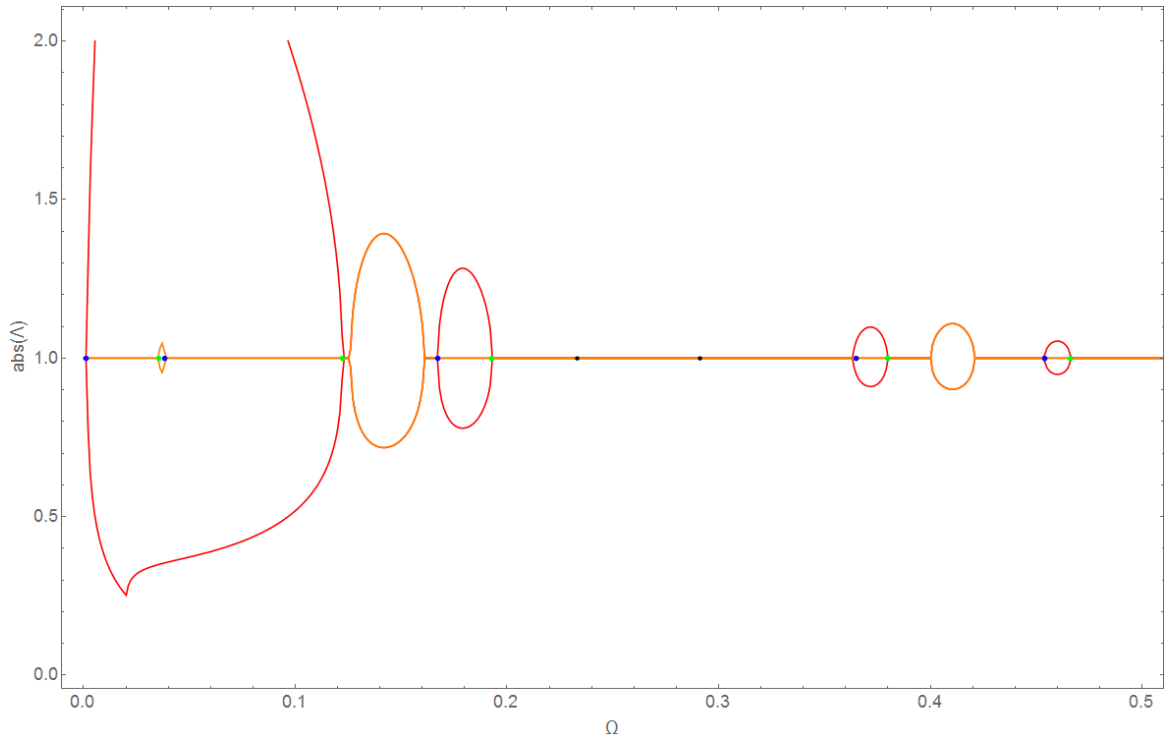

Figure 3.16: Eigenfrequencies of three periodicity cell border conditions A (red) and border conditions B (green), common EF - black

Out-plane vibrations shows the same picture and therefore, for brevity it is not shown. As seen, properties of eigenfrequencies, considered in [7], [8] and Ch.2 are preserves for Bernoulli-Euler ring case.

3.3.3 Eigenmodes analysis

Eingenmode analysis gives clear understanding of wave propagation picture in infinite waveguide. Form of waves and energy transmission mode (standing or propagating wave) can be easily shown when eigenmodes analysis is performed. Also it is first step to strain state analysis, which is often of interest in engineering practice.

First same procedure used and determinant $D(\Lambda, \Omega)$ obtained from system Eq.3.31a-Eq.3.32b. As shown above in case of a flat ring second branch of Floquet zones appears. And difference between full and partial gap-band can be considered (see Fig.3.12).

For each root of polynomial $D^{in}(\Lambda, \Omega)$ one can find eigenmodes of in-plane vibrations. System Eq.3.31a-Eq.3.32b with parameter Λ substituted has zero determinant. Therefore, one constant assumed as constant, for example $u_1(0) = 1$ and one arbitrary of equations of the system excluded from consideration. For certainty system Eq.3.31a-Eq.3.32b with first equation changed to $u_1(0) = 1$ called eigenmode of infinite waveguide. In the pure gap-band all waves are standing:

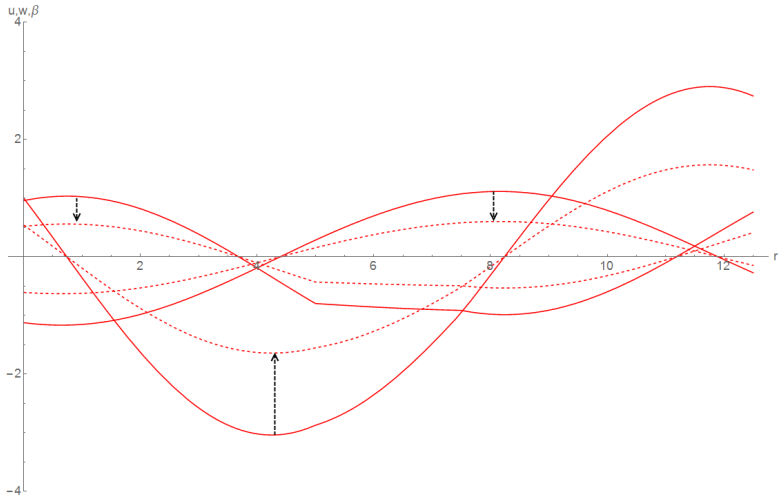

Figure 3.17: Standing waves in pure gap-band $\Omega = 0.037$

In all cases all waved coupled as increasing-evanescent or traveling from left to right and right-left in three groups such that $\Lambda_1 * \Lambda_2 = 1$. In partial gap-band appears one pair of propagating travelling waves, whereas other two pairs are standing and coupled as increasing-evanescent:

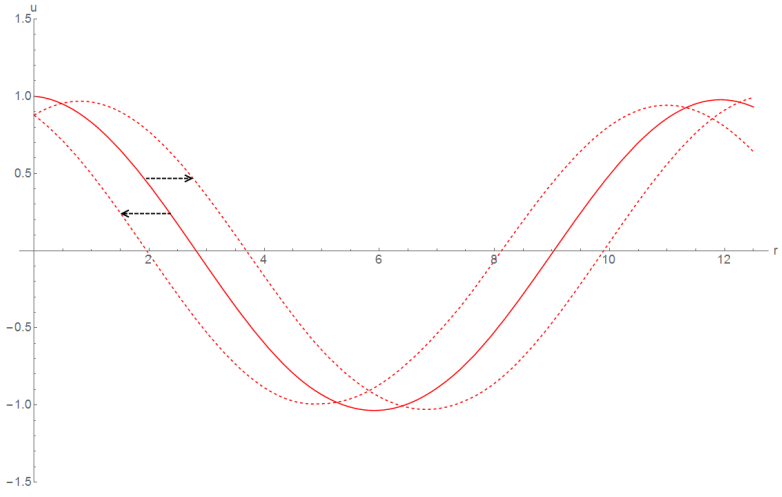

Figure 3.18: One pair of travelling waves in partial gap-band $\Omega = 0.06$

And in pure pass-band appears second couple of travelling propagating waves and one couple standing increasing-evanescent. Waves for pass-band will not be represented here for brevity.

3.4 The spatial periodic structure

Parts of model, shown on a Fig.3.10 are connected such that plane of in-plane vibrations of first part is perpendicular to a plane of in-plane vibrations of the second part. Whereas boundary integrals are not affected by such kind of rotation of coordinate system, interfacial conditions are changing due to local coordinate system in different parts:

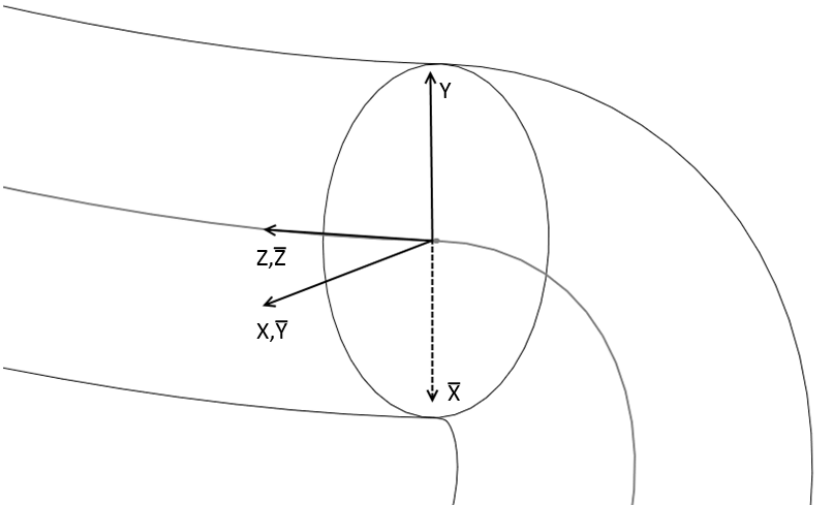

Figure 3.19: Local coordinate systems

Coordinate change is rotation on the angle $\pi/2$ with respect to z axis. Therefore, interfacial conditions changing as:

$$\begin{array}{l} u = \bar{v},\ v = -\bar{u},\ w = \bar{w} \\ \alpha = -\bar{\beta},\ \beta = -\bar{\alpha},\ \gamma = \bar{\gamma} \end{array} \tag{3.36}$$

With this coordinate changing new displacement and force vector definitions are required

$$\begin{array}{l} disp_{i1}(s) = \{w_{i1}(s), \beta_{i1}(s), u_{i1}(s), v_{i1}(s), \gamma_{i1}(s), \alpha_{i1}(s)\} \\ force_{i1}(s) = \frac{1}{E_i I_x^{i1}}\{Q_x^{i1}(s), N_z^{i1}(s), M_y^{i1}(s), Q_y^{i1}(s), M_x^{i1}(s), T_z^{i1}(s)\} \\ disp_{i2}(s) = \{w_{i2}(s), -\alpha_{i2}(s), v_{i2}(s), -u_{i2}(s), \gamma_{i2}(s), -\beta_{i2}(s)\} \\ force_{i2}(s) = \frac{1}{E_i I_x^{i2}}\{Q_y^{i2}(s), N_z^{i2}(s), -M_x^{i2}(s), -Q_x^{i2}(s), -M_y^{i2}(s), T_z^{i2}(s)\} \end{array} \tag{3.37}$$

,where $i1 = 1, 3, 5, ...$ are parts with odd numbers and $i2 = 2, 4, 6, ...$ are parts with even numbers. Parts are coupled with respect to geometry.

With this new definition Floquet problem can be defined as above:

$$\begin{array}{l} w_1(1) = w_2(1)\ ; \beta_1(1) = -\alpha_2(1)\ ; u_1(1) = v_2(1) \\ \gamma_1(1) = \gamma_2(1)\ ; v_1(1) = -u_2(1)\ ; \alpha_1(1) = -\beta_2(1) \\ N_z^{(1)}(1) = \alpha_{par}\, N_z^{(2)}(1)\ ; M_y^{(1)}(1) = -\alpha_{par}\, M_x^{(2)}(1)\ ; Q_x^{(1)}(1) = \alpha_{par}\, Q_y^{(2)}(1) \\ T_z^{(1)}(1) = \alpha_{par}\, T_z^{(2)}(1)\ ; Q_y^{(1)}(1) = -\alpha_{par}\, Q_x^{(2)}(1)\ ; M_x^{(1)}(1) = -\alpha_{par}\, M_y^{(2)}(1) \\ w_2(1+\gamma_{par}) = w_3(1+\gamma_{par})\ ; \beta_2(1+\gamma_{par}) = -\alpha_3(1+\gamma_{par})\ ; u_2(1+\gamma_{par}) = v_3(1+\gamma_{par}) \\ \gamma_2(1+\gamma_{par}) = \gamma_3(1+\gamma_{par})\ ; v_2(1+\gamma_{par}) = -u_3(1+\gamma_{par})\ ; \alpha_2(1+\gamma_{par}) = -\beta_3(1+\gamma_{par}) \\ N_z^{(2)}(1+\gamma_{par}) = \alpha_{par}\, N_z^{(3)}(1+\gamma_{par})\ ; M_y^{(2)}(1+\gamma_{par}) = -\alpha_{par}\, M_x^{(3)}(1+\gamma_{par}) \\ Q_x^{(2)}(1+\gamma_{par}) = \alpha_{par}\, Q_y^{(3)}(1+\gamma_{par}) \\ T_z^{(2)}(1+\gamma_{par}) = \alpha_{par}\, T_z^{(3)}(1+\gamma_{par})\ ; Q_y^{(2)}(1+\gamma_{par}) = -\alpha_{par}\, Q_x^{(3)}(1+\gamma_{par}) \\ M_x^{(2)}(1+\gamma_{par}) = -\alpha_{par}\, M_y^{(3)}(1+\gamma_{par}) \end{array}$$

(3.38a)

Or in vector form:

$$\begin{aligned} &disp_1(1) = disp_2(1) \\ &force_1(1) = \alpha\, force_2(1) \\ &disp_2(1+\gamma) = disp_3(1+\gamma) \\ &\alpha force_2(1+\gamma) = force_3(1+\gamma) \\ &disp_1(0) = \Lambda\, disp_3(1+\gamma) \\ &force_1(0) = \Lambda\, force_3(1+\gamma) \end{aligned} \tag{3.38b}$$

System of equations Eq.3.38b with definitions Eq.3.37 is define system of linear algebraic equations. Determinant of this system $\bar{D}(\Lambda, \Omega)$ is the twelfth order polynomial, which also factorizes into two six-order parts $\bar{D}(\Lambda, \Omega) = \bar{D}^{w,v}(\Lambda, \Omega) * \bar{D}^{\gamma,u}(\Lambda, \Omega)$. But, since we consider essentially spatial structure, one can not divide vibrations into in-plane and out-plane mode because vibrations plane can't be defined for spatial structures. Dependence Λ of Ω also can be plotted as:

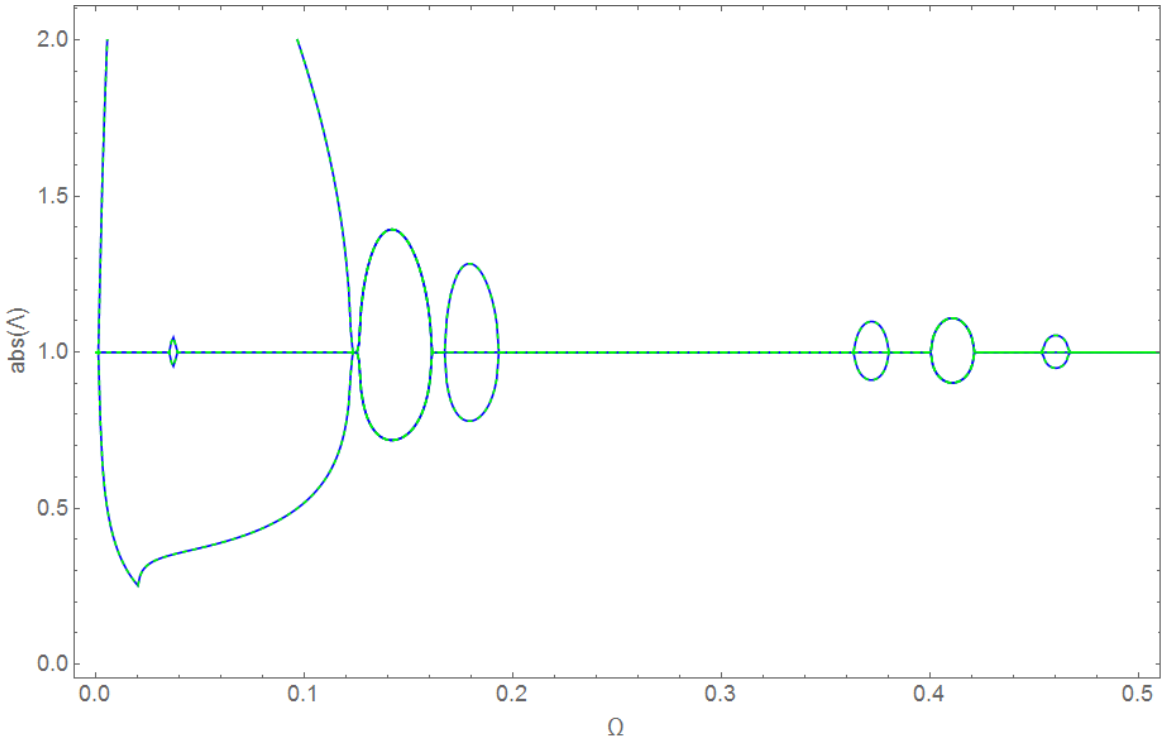

Figure 3.20: Floquet zones of $D^{w,u}(\Lambda, \Omega)$(blue) and $\bar{D}^{w,v}(\Lambda, \Omega)$(green)

As seen, both pictures are matching. This is explained by natural symmetry of problem considered, both in-plane and out-plane displacement have same stiffness and therefore their interchange does not affect end result. Parts $D^{\gamma,v}(\Lambda, \Omega)$ and $\bar{D}^{\gamma,u}(\Lambda, \Omega)$ also matching and therefore not represented here.

Thus, auxiliary problem are exact correspond to model, shown on a Fig.3.2. And all results, shown above are valid for a first model.

3.5 Parametric study

In engineering application often of interest to know, how a parameter's change affects on properties of system. It is used in optimization process in order to choose proper methods for optimization and reach best possible optimal properties.

Recalling initial parameters:

$$\alpha = 1; \gamma_1 = 0.5;\ \sigma = 1; \lambda = 5;\ \varepsilon_1 = 0.2;\ \varepsilon_2 = 0.02 \tag{3.39}$$

First, let us consider part curvature ratio $\bar{\epsilon} = \frac{\epsilon_1}{\epsilon_2}$ change effect. For parameters considered above it has value of $\bar{\epsilon}_1 = \frac{0.2}{0.02} = 10$. For determinacy parameter ϵ_2 is fixated and influence of changing ϵ_1 on Floquet zones picture is considered.

On the plot below with no color shown full gap bands for a given parameter $\bar{\epsilon}$ and given frequency Ω, whereas color represents partial or full pass band:

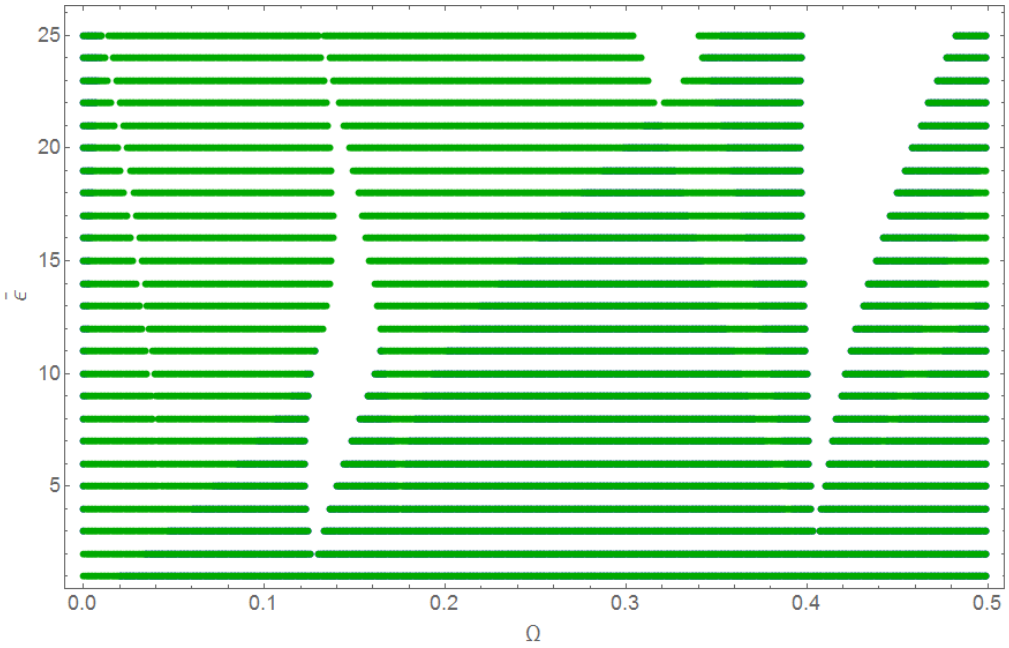

Figure 3.21: Floquet zones for different $\bar{\epsilon}$

As seen, with increasing ratio $\bar{\epsilon}$ pure gap bands tends to move to higher frequency.

Second parameter considered is γ, following plot also represents full gap bands and partial or full pass bands as above:

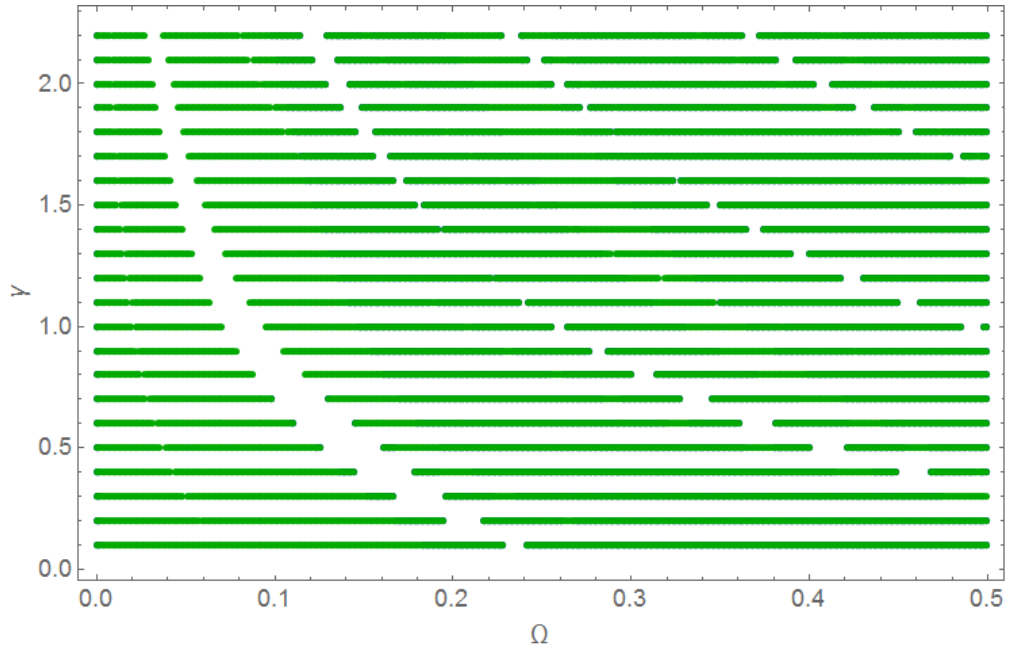

Figure 3.22: Floquet zones for different γ

For γ we have reciprocal tendency, with increasing γ gap bands tends to move to lower frequency.

This parameter study in showing that model considered can be used for engineering applications for optimization processes and obtaining properties, demanded by the industry and considering basic ideas of influence of parameters on pure gap band positions.

In this chapter first model of a torque vibration isolator was considered. It has been modelled as a system of differential equations for an infinite periodic structure. Therefore, methods, used in Ch.2, were expanded to a system of a differential equation. Green's matrix coefficient with using bi-orthogonality condition were obtained in analytical form. Difference between Floquet zones of a single differential equation and system of differential equation was shown. Also, was shown independence with respect to symmetry transformation of Floquet zones for a structure with natural symmetry. Also parameters study was conducted in order to show one of industrial applications of given model.

Conclusion and future work

First part of this master project has two main goals: theoretical and practical. In practical point of view torque simple vibration isolator model was considered and vibration isolation properties of this structure were considered. Model shows that full waves propagation block can be reached in low frequency region, that of interest in industrial applications. Also, possibility of model optimization was shown, but deep investigation of optimization of properties are out of scope of this project.

From theoretical point of view, all main principles of Floquet theory have been developed and shown on examples. Possibility of using of polar coordinates were considered. Also first step in hierarchy of torque vibration isolator models were considered. Model of torque vibration isolator has been developed and considered in frame of Floquet zones theory. Tools that developed in this part of master's project have broad range of applicability and they will be used in second part of work. Results obtained in this part will be used for comparison with second model, which will be considered in second part of master's project.

One of supplementary goals was to develop and validate the program that can be used for modelling of an isolator. Wolfram Mathematica software was used for programming, because it fits best for analytical modelling.

Also, first parts gives all necessary theory, shown in examples and with all necessary references, that allows one to use differential equations in modelling of vibrations of physical structures.

Goal reached in this part, gives following propositions for goals of second part:

(I) Consider second model circular plate-cylindrical shell, using developed for polar coordinate system Floquet theory from theoretical and practical point of view

(II) Compare first and second model in order to consider advantages and disadvantages of choice of more complicated model. Also it is of interest in theoretical point of view to compare Floquet theory for different coordinate system.

(III)Conduct experiments in order to validate models and developed theory and define practical applicability of considered in both parts of masters's project models

Both parts allows one to build hierarchy of two models of torque vibration isolator, that uses wide range of methods with wide range of applicability.

Literature

1. L.Brillouin. Wave Propagation in Periodic Structures second ed. Dover Publications New York, 1953.
2. D.J.Mead. Wave propagation in continuous periodic structures. Research contributions from Southampton 1964-1995 // Journal of Sound and Vibration. 1996. Vol. 190. P. 495–524.
3. A.Søe-Knudsen, R.Darula, Sorokin S. Theoretical and experimental analysis of the stop-band behavior of elastic springs with periodically discontinuous of curvature // Journal of the Acoustical Society of America. 2012. Vol. 132. P. 1378–1383.
4. A.Søe-Knudsen, Sorokin S. Modelling of linear wave propagation in spatial fluid filled pipe systems consisting of elastic curved and straight elements // Journal of Sound and Vibration. 2010. Vol. 329. P. 5116–5146.
5. A.Søe-Knudsen. Design of stop-band filter by use of curved pipe segments and shape optimization // Structural and Multidisciplinary Optimization. 2011. Vol. 44. P. 863–874.
6. A.Søe-Knudsen. Design of stop-band filters by use of compound curved pipe segments and shape optimization // 10th International Conference on Recent Advances in Structural Dynamics. Institute of Sound and Vibration Research, 2010.
7. A.Hvatov, S.Sorokin. Analysis of eigenfrequencies of finite periodic structures in view of location of frequency pas- and stop-bands // Proceedings of 20th International Congress on Sound and Vibration. 2013.
8. A.Hvatov, S.Sorokin. Free vibrations of finite periodic structures in pass- and stop-bands of the counterpart infinite waveguides // Journal of Sound and Vibration. 2015. Vol. 347. P. 200–217.
9. S.Sorokin. On the bi-orthogonality conditions for multi-modal elastic waveguides. // Journal of Sound and Vibration. 2013. Vol. 332. P. 5606–5617.
10. Dym C. L., I.H.Shames. Solid Mechanics. A Variational Approach, Augmented Edition. Springer, 2013.
11. Duffy D. G. Green's Functions with Applications. Chapman and Hall, 2001.
12. Skudrzyk E. The Foundations of Acoustics. Basic mathematics and basic acoustics. Springer-Verlag, 1971.
13. Achenbach J. D. Reciprocity in Elastodynamics. Cambridge University Press, 2003.
14. S.Sorokin. The Green's matrix and the boundary integral equations for analysis of time-harmonic dynamics of elastic helical springs. // Journal of the Acoustical Society of America. 2011. Vol. 129. P. 1315–1323.
15. R.Nielsen, S.Sorokin. Periodicity effects of axial waves in elastic compound rods // Journal of Sound and Vibration. 2015. Vol. 353. P. 135–149.

Appendix A

Derivation of equation of motion for a circular membrane

Kinetic energy is written in form

$$T = \frac{1}{2}\iint_S \rho u_t^2 dS \tag{A.1}$$

Potential energy is written in form

$$V = \frac{1}{2}\iint_S T_0(u_x + u_y)dS + \frac{1}{2}\int_L \sigma(L)u^2 dL \tag{A.2}$$

where $T_0 = const$ membrane surface tension,
$\sigma(L)$ membrane elasticity module.

Action integral have form:

$$H = \frac{1}{2}\int_{t_0}^{t_1}\iint_S (T-V)dSdt = \frac{1}{2}\int_{t_0}^{t_1}(\iint_S(\rho u_t^2 - T_0(u_x+u_y))dS - \frac{1}{2}\int_L \sigma(L)u^2 dL)dt \tag{A.3}$$

Variation of the first summand:

$$\int_{t_0}^{t_1}\iint_S \rho u_t \delta u_t dSdt = \iint_S \rho u_t \delta u\big|_{t_0}^{t_1} dS - \int_{t_0}^{t_1}\iint_S \rho u_t \delta u_t t \delta u dSdt = -\int_{t_0}^{t_1}\iint_S \rho u_{tt}\delta u dSdt \tag{A.4}$$

Second summand:

$$-\int_{t_0}^{t_1}\iint_S T_0 u_x \delta u_x dSdt = -\int_{t_0}^{t_1}\int_L T_0 u_x \delta u dy dt + \int_{t_0}^{t_1}\iint_S T_0 u_{xx}\delta u dSdt \tag{A.5}$$

Third summand:

$$-\int_{t_0}^{t_1}\iint_S T_0 u_y \delta u_y dSdt = -\int_{t_0}^{t_1}\int_L T_0 u_y \delta u dx dt + \int_{t_0}^{t_1}\iint_S T_0 u_{yy}\delta u dSdt \tag{A.6}$$

With $u_x dy + u_y dx = \frac{du}{dn}$ first parts of A.5 and A.6 turns to:

$$-\int_{t_0}^{t_1}\int_L T_0 \frac{du}{dn}\delta u dL dt \tag{A.7}$$

Total variation δH from A.4-A.7

$$\delta H = \int_{t_0}^{t_1} \int_L (\sigma(L)u - T_0 \frac{du}{dn}) \delta u dL dt + \int_{t_0}^{t_1} \iint_S (T_0(u_{xx} + u_{yy}) - \rho u_{tt}) \delta u dS dt \tag{A.8}$$

From which we obtain membrane equation of motion:

$$T_0 \Delta u - \rho u_{tt} = 0 \tag{A.9}$$

And two possibly border conditions

$$(\sigma(L)u - T_0 \frac{du}{dn})\Big|_L = 0 \tag{A.10}$$

or

$$u\Big|_L = 0 \tag{A.11}$$

With time dependence $\exp(-i\omega t)$, i.e. $u(\mathbf{x}, t) = U(\mathbf{x}) \exp(-i\omega t)$ equation A.9 can be rewritten as:

$$\Delta U + \frac{\omega^2 \rho}{T_0} U = 0 \tag{A.12}$$

And with designation $k^2 = \frac{\omega^2 \rho}{T_0}$ it has final form (uppercase omitted):

$$(\Delta + k^2)u = 0 \tag{A.13}$$

It should be empathized, that potential energy has the form:

$$V = \frac{1}{2} \iint_S (T_0 + EA)(u_x + u_y) dS + \frac{1}{2} \int_L \sigma(L) u^2 dL \tag{A.14}$$

And when limit $EA \to 0$ considered one has pure membrane vibrations case. Otherwise, $EA >> T_0$ represents plate in-plane vibration case. Here limit $EA \to 0$ considered from beginning.

Appendix B

Derivation of the boundary integral equation for a circular membrane

Starting with following equation

$$u''(r) + \frac{1}{r}u(r) + \left(k^2 - \frac{m^2}{r^2}\right)u(r) = -q(r) \tag{B.1}$$

Multiplying by $G(r, r_0)$ and integrating over all membrane area gives:

$$I = \int_0^{2\pi}\int_a^b (u''(r) + \frac{1}{r}u(r) + \left(k^2 - \frac{m^2}{r^2}\right)u(r))G(r, r_0)rdrd\phi = -\int_0^{2\pi}\int_a^b q(r)G(r, r_0)rdrd\phi \tag{B.2}$$

Since axi-symmetric case considered:

$$I = 2\pi\int_a^b (u''(r) + \frac{1}{r}u(r) + \left(k^2 - \frac{m^2}{r^2}\right)u(r))G(r, r_0)rdr = -2\pi\int_a^b q(r)G(r, r_0)rdr \tag{B.3}$$

And after cancellation:

$$I = \int_a^b (u''(r) + \frac{1}{r}u(r) + \left(k^2 - \frac{m^2}{r^2}\right)u(r))G(r, r_0)rdr = -\int_a^b q(r)G(r, r_0)rdr \tag{B.4}$$

Considering following integrals and using by-part integration (arguments omitted for brevity and clarity):

$$I_1 = \int_a^b u''\,G\,r dr = u'\,G\,r\Big|_a^b - \int_a^b u'(\,G'\,r + G)dr = [u'\,G\,r - u(\,G'\,r + G)]\Big|_a^b + \int_a^b u(G' + G' + G''\,r)dr \tag{B.5}$$

$$I_2 = \int_a^b u'\,G\,dr = u\,G\Big|_a^b - \int_a^b u\,G'\,dr \tag{B.6}$$

$$I_3 = \int_a^b \left(k^2 - \frac{m^2}{r^2}\right) u\, G\, r dr \tag{B.7}$$

Substituting B.5-B.7 into B.4 gives:

$$I = I_1 + I_2 + I_3 = [u'\, G\, r - u\, G'\, r]\Big|_a^b + \int_a^b (G'' + \frac{1}{r}G' + \left(k^2 - \frac{m^2}{r^2}\right) G) u\, r dr \tag{B.8}$$

Recalling modified Green's function definition:

$$G''(r, r_0) + \frac{1}{r}G'(r, r_0) + \left(k^2 - \frac{m^2}{r^2}\right) G(r, r_0) = -\frac{\delta(r - r_0)}{r_0} \tag{B.9}$$

With definition B.9 equation B.8 has the form:

$$I = [u'(r)\, G(r, r_0) - u(r)\, G'(r, r_0)] r\Big|_{r=a}^{r=b} + \int_a^b -\frac{\delta(r - r_0)}{r_0} u(r)\, r dr \tag{B.10}$$

And with property of delta function it can be rewritten as:

$$I = [u'(r)\, G(r, r_0) - u(r)\, G'(r, r_0)] r\Big|_{r=a}^{r=b} - \frac{u(r_0)\, r_0}{r_0} \tag{B.11}$$

Here modified Green's function used, in term $\frac{u(r_0)\, r_0}{r_0}$ cancelled r_0 and boundary equation has more simple form.Also, it can be rewritten with recalled right hand side of B.4 in form:

$$u(r_0) = [u'(r)\, G(r, r_0) - u(r)\, G'(r, r_0)] r\Big|_{r=a}^{r=b} + \int_a^b q(r) G(r, r_0) dr \tag{B.12}$$

Appendix C

Axial rod vibrations in boundary equations method point of view

C.1 Green's function definition and derivation

Axial beam vibration can be described with following equation:

$$u_{xx} - \frac{1}{c^2}u_{tt} = -q(x,t) \tag{C.1}$$

,where c has meaning of sound of speed (speed of elastic wave propagation) and q(x,t) is the force density.

With harmonic vibrations state assumed $u(x,t) = \exp[(-i\omega t)U(x)$ Eq.C.1 can be rewritten as:

$$u''(x) + k^2 u(x) = -q(x) \tag{C.2}$$

,where $k = \frac{\omega}{c}$ called wave number. In what follows harmonic vibrations state assumed and uppercase of letters is omited.

Green's function by definition is a solution of the equation with force density $q(x) = \delta(x - x_0)$, where $\delta(x)$ is Dirac's delta function. In the rod axial vibrations case it has meaning of a point force acting at point x with observation point x_0 and Green's function equation can be written as:

$$\frac{d^2}{dx^2}G(x,x_0) + k^2 G(x,x_0) = -\delta(x - x_0) \tag{C.3}$$

It can be proven that Green's function should satisfy following properties:

$$\begin{array}{l} G(x,x_0) = G(x_0,x) \\ \frac{\partial}{\partial x}G(x_0,x_0+\varepsilon) - \frac{\partial}{\partial x}G(x_0,x_0-\varepsilon) = -1,\ \varepsilon \to 0 \\ G(x_0,x_0+\varepsilon) = G(x_0,x_0-\varepsilon),\ \varepsilon \to 0 \end{array} \tag{C.4}$$

Since common solution of homogenous equation C.2 has the form:

$$u(x) = C_1 \exp(ikx) + C_2 \exp(-ikx) \tag{C.5}$$

Solution of equation can be written in form (if one should consider infinite beam it is very important that function $G(x,x_0)$ should satisfy radiation conditions at infinity [12]):

$$\begin{array}{l} G_+(x,x_0) = A\ \exp(ikx)\,, x > x_0 \\ G_-(x,x_0) = B\ \exp(-ikx)\,, x \le x_0 \end{array} \tag{C.6}$$

Green's function in form Eq.C.6 substituted into two last properties in C.4 gives:

$$\begin{aligned} &G_+(x_0,x_0) = G_-(x_0,x_0) \\ &\tfrac{d}{dx}(G_+(x,x_0) - G_-(x,x_0))\Big|_{x=x_0} = -1 \end{aligned} \tag{C.7}$$

or in explicit form:

$$\begin{aligned} &A\ \exp(ikx_0) = B\ \exp(-ikx_0) \\ &ikA\exp(ikx_0) + ikB\exp(-ikx_0) = -1 \end{aligned} \tag{C7'}$$

System Eq.C7' has the unique solution for unknown coefficients A and B:

$$\{A,B\} = \{\frac{i}{2k}\exp(-ikx_0), \frac{i}{2k}\exp(ikx_0)\} \tag{C.8}$$

And finally Green's function can be written as:

$$G(x,x_0) = \begin{cases} \frac{i}{2k}\exp(-ik(x-x_0)) & x \le x_0 \\ \frac{i}{2k}\exp(ik(x-x_0)) & x > x_0 \end{cases} \tag{C.9}$$

Or in short form:

$$G(x,x_0) = \frac{i}{2k}\exp(ik\ \text{abs}(x-x_0)) \tag{C.10}$$

If this function plotted it is seen that all properties Eq.C.4 are fulfilled:

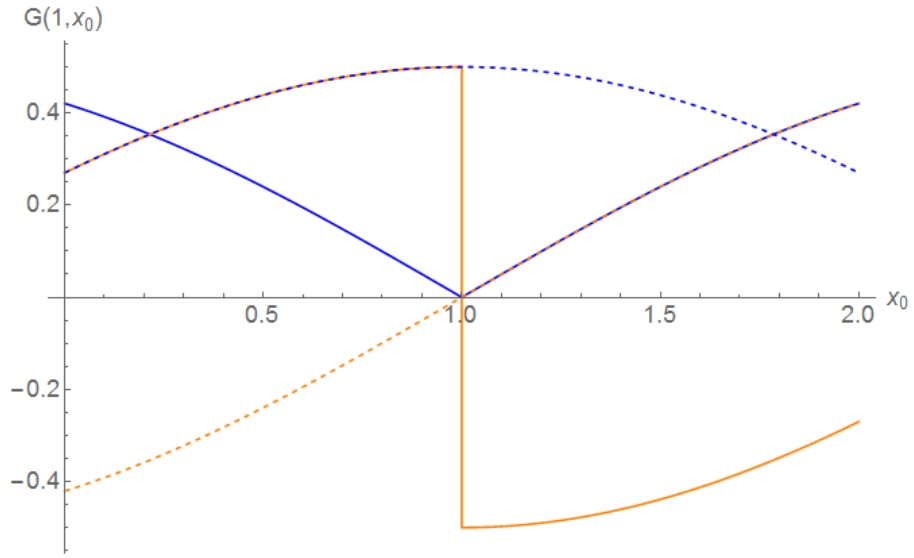

Figure C.1: Green's function of axial rod vibration equation(blue) and its derivative(orange) and imaginary parts (dashed)

C.2 Equation of axial displacement of a rod. Boundary integrals method

Green's function can be used in order to obtain solution of a differential equation with arbitrary load. Recalling axial rod vibrations equation:

$$u''(x) + k^2u(x) = -q(x) \tag{C.11}$$

And Green's function definition:

$$\frac{d^2}{dx^2}G(x,x_0) + k^2 G(x,x_0) = -\delta(x-x_0) \tag{C.12}$$

In what follows $\frac{d}{dx}G(x,x_0) = G'(x,x_0)$
Multiplying equation C.11 on $G(x,x_0)$ and integrating over beam length

$$\int_a^b (u''(x) + k^2 u(x))G(x,x_0)dx = -\int_a^b q(x)G(x,x_0)dx \tag{C.13}$$

First left hand side of an equation C.13 considered:

$$I = \int_a^b (u''(x) + k^2 u(x))G(x,x_0)dx \tag{C.14}$$

Considering following integral and using by-part integration:

$$\begin{aligned} I_1 &= \int_a^b u''(x)G(x,x_0)dx = u'(x)G(x,x_0) - \int_a^b u'(x)G'(x,x_0)dx = \\ &= [u'(x)G(x,x_0) - u(x)G'(x,x_0)]\Big|_a^b + \int_a^b u(x)G''(x,x_0)dx \end{aligned} \tag{C.15}$$

And second part of integral just rewritten as:

$$I_2 = \int_a^b k^2 u(x)G(x,x_0)dx \tag{C.16}$$

With using equality $I = I_1 + I_2$ Eq.C.14 can be rewritten:

$$I = [u'(x)G(x,x_0) - u(x)G'(x,x_0)]\Big|_a^b + \int_a^b (G''(x,x_0) + k^2 G(x,x_0))u(x)dx \tag{C.17}$$

With Green's function definition Eq.C.12 one can rewrite equation C.17 in form:

$$I = [u'(x)G(x,x_0) - u(x)G'(x,x_0)]\Big|_a^b - \int_a^b \delta(x-x_0)u(x)dx \tag{C.18}$$

Dirac's delta-function has a property:

$$\int_a^b f(x)\delta(x-x_0)dx = f(x_0) \tag{C.19}$$

,which is valid for any range (a,b) that contains x_0 including $(-\infty,+\infty)$.
With property C.19 and recalling right hand side of C.13 one can rewrite C.18

$$u(x_0) = [u'(x)G(x,x_0) - u(x)G'(x,x_0)]\Big|_a^b + \int_a^b q(x)G(x,x_0)dx \tag{C.20}$$

Therefore, if values on a beam boundary are known, one can find displacement at any point within the boundary. Eq.C.20 is called boundary integral equation for an axial rod vibrations.

C.3 Boundary integrals method direct application

Let us consider unit length beam with forcing problem written as:

$$\begin{aligned} u(0) &= 1 \\ u(1) &= 0 \end{aligned} \tag{C.21}$$

For brevity no external loading considered, i.e. $q(x) \equiv 0$. For both boundaries boundary integral should be written as:

$$\begin{aligned} u(0) &= (u'(1)G(1,0) - u(1)G'(1,0)) - (u'(0)G(0,0) - u(0)G'(0,0)) \\ u(1) &= (u'(1)G(1,1) - u(1)G'(1,1)) - (u'(0)G(0,1) - u(0)G'(0,1)) \end{aligned} \tag{C.22}$$

Or in implicit form :

$$\begin{aligned} &\tfrac{1}{2}u(0) - \tfrac{1}{2}\exp(ik)u(1) + \tfrac{i}{2k}u1(0) - \tfrac{i\exp(ik)}{2k}u1(1) = 0 \\ &-\tfrac{1}{2}\exp(ik)u(0) + \tfrac{1}{2}u(1) + \tfrac{i\exp(ik)}{2k}u1(0) - \tfrac{i}{2k}u1(1) = 0 \end{aligned} \tag{C.23}$$

,where $u(0), u(1), u'(0), u'(1)$ are yet unknown. With boundary conditions added following system has the unique solution:

$$\begin{aligned} &\tfrac{1}{2}u(0) + \tfrac{1}{2}\exp(-ik)u(1) + \tfrac{i}{2k}u1(0) - \tfrac{i\exp(-ik)}{2k}u1(1) = 0 \\ &\tfrac{1}{2}\exp(-ik)u(0) + \tfrac{1}{2}u(1) + \tfrac{i\exp(-ik)}{2k}u1(0) - \tfrac{i}{2k}u1(1) = 0 \\ &u(0) = 1 \\ &u(1) = 0 \end{aligned} \tag{C.24}$$

It can be found as:

$$\{u(0), u(1), u'(0), u'(1)\} = \{1, 0, (2 - i\cot(k))ik, -i\frac{ik}{\sin(k)}\} \tag{C.25}$$

After found constants Eq.C.25 are substituted into Eq.C.20 and displacement can be obtained for any point x_0 within the range (0,1) (here $k \equiv 1$):

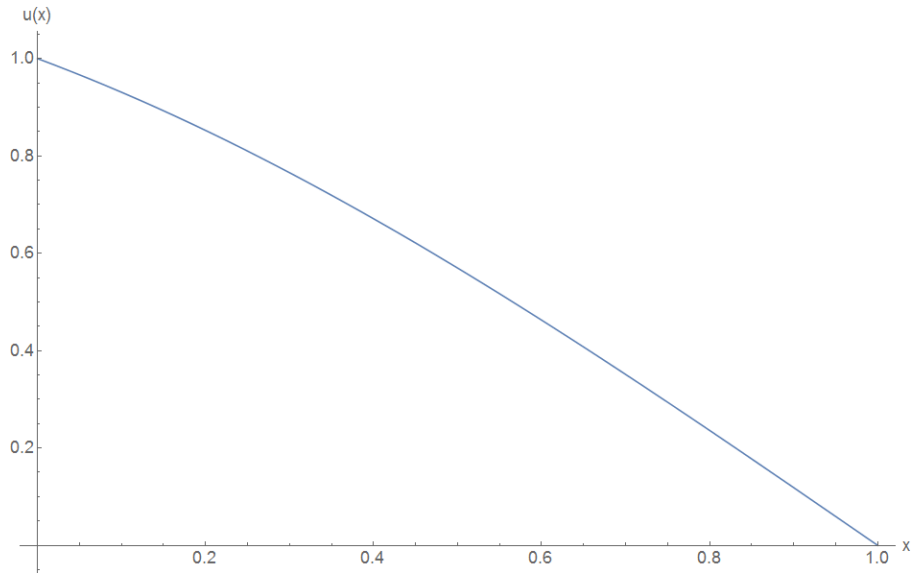

Figure C.2: Displacement found with boundary integrals

This solution can be validated trough transfer matrix method. This method has less computation difficulty, but also less stabile. In axial rod vibrations case it gives significant computational advantage, but in other cases stability question should be considered.

Recalling axial rod vibration equation (here also $q(x) \equiv 0$):

$$u''(x) + k^2 u(x) = 0 \tag{C.26}$$

It has common solution in form:

$$u(x) = C_1 \exp(ikx) + C_2 \exp(-ikx) \tag{C.27}$$

And considering same boundary problem Eq.C.23 one can write following system:

$$\begin{aligned} u(0) &= C_1 + C_2 = 1 \\ u(1) &= C_1 \exp(ik) + C_2 \exp(-ik) = 0 \end{aligned} \tag{C.28}$$

System Eq.C.28 can be solved with respect to unknown integration constaints C_1, C_2 as:

$$\{C_1, C_2\} = \{\frac{1}{1 - \exp(2i)}, \frac{1}{1 - \exp(-2i)}\} \tag{C.29}$$

When constants Eq.C.29 are substituted into C.27 displacement can be plotted as:

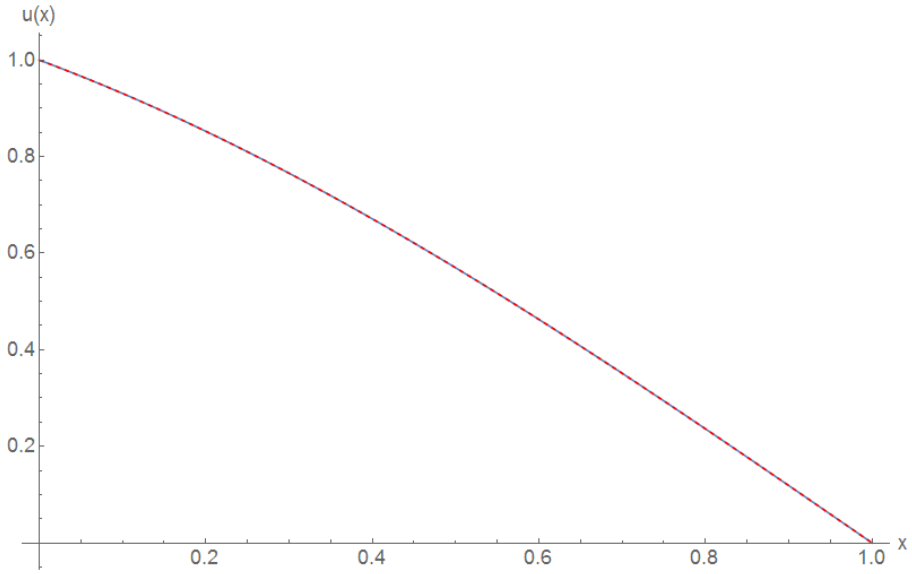

Figure C.3: Displacement found with boundary integrals(blue) and displacement found by transfer matrix method (red)

As seen, both methods are giving the same result. Advantage of the boundary integrals method are not seen here, but in more complicated cases which are considered in main part instability of a transfer matrix method is significant and it can not be used for obtaining results. Still,it were used for checking validity of found Green's functions.

Appendix D

Floquet theorem. Infinite periodic rod.

Floquet theorem is a very powerful tool for finding solution for a differential equations on a infinite periodic structures. This is very common theorem for a periodic differential operator and lies out of scope of this work. Nevertheless, it will be shown here for a particular case. Here an infinite periodic rod axial vibrations case will be considered. Results of this chapter is used in Ch.1 for comparison

Infinite rod can be represented as:

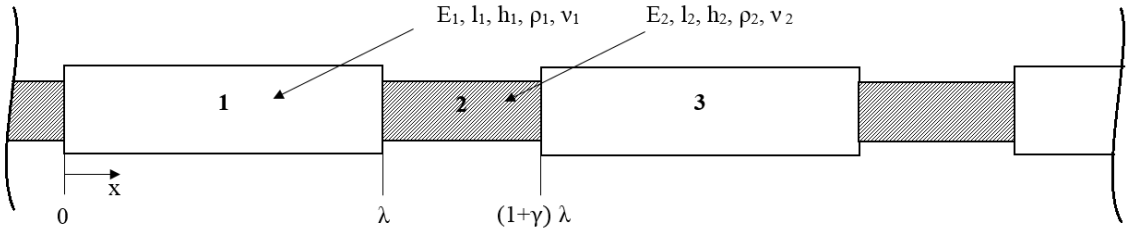

Figure D.1: Infinite rod

Each part of rod has its own vibration equation written as (harmonic vibrations state assumed and also, for brevity free vibrations state, i.e. $q(x) \equiv 0$ for any part of infinite rod):

$$\begin{array}{l} u_1''(x) + k_1^2 u_1(x) = 0 \\ u_2''(x) + k_2^2 u_2(x) = 0 \\ \ldots \\ u_n''(x) + k_n^2 u_n(x) = 0 \\ \ldots \end{array} \tag{D.1}$$

In this appendix following dimensionless parameters are used:

$$\alpha = \frac{E_2}{E_1}; \beta = \frac{h_2}{h_1}; \gamma = \frac{l_2}{l_1}; \sigma = \frac{c_2}{c_1}; \lambda = \frac{l_1}{h_1}; \Omega = \frac{\omega h_1}{c_1} \tag{D.2}$$

Since we have only two kind of sections "white"and "black"we are interested only in two equations (all quantities are already dimensionless):

$$\begin{array}{l} u_{white}''(x) + \Omega^2 u_{white}(x) = 0 \\ u_{black}''(x) + (\frac{\Omega\beta}{\sigma})^2 u_{black}(x) = 0 \end{array} \tag{D.3}$$

,where $white = 1, 3, 5, ...$ are number of section with first set of parameters and $black = 2, 4, 6, ...$ are number of sections with second set of parameters.

For each section one can find Green's function in form Eq.C.10:

$$\begin{array}{c} G_{white}(x,x_0) = \frac{i}{2\Omega}\exp(-i\Omega\,\mathrm{abs}(x-x0)) \\ G_{black}(x,x_0) = \frac{i\sigma}{2\Omega\beta}\exp(-i\frac{\Omega\beta}{\sigma}\,\mathrm{abs}(x-x0)) \end{array} \tag{D.4}$$

And boundary integrals in form Eq.C.20 respectively:

$$u_i(x_0) = [u_i'(x)G_i(x,x_0) - u_i(x)G_i'(x,x_0)]\Big|_{a_i}^{b_i} \tag{D.5}$$

Let's consider three consequent parts of infinite rod (they are marked with numbers on a Fig.D.1). For each boundary boundary integrals can be written:

$$\begin{array}{l} u_1(0) = (u_1'(\lambda)G_1(\lambda,0) - u_1(\lambda)G_1'(\lambda,0)) - (u_1'(0)G_1(0,0) - u_1(0)G_1'(0,0)) \\ u_1(\lambda) = (u_1'(\lambda)G_1(\lambda,\lambda) - u_1(\lambda)G_1'(\lambda,\lambda)) - (u_1'(0)G_1(0,\lambda) - u_1(0)G_1'(0,\lambda)) \\ u_2(\lambda) = (u_2'((1+\gamma)\lambda)G_2((1+\gamma)\lambda,\lambda) - u_2((1+\gamma)\lambda)G_2'((1+\gamma)\lambda,\lambda)) - \\ -(u_2'(\lambda)G_2(\lambda,\lambda) - u_2(\lambda)G_2'(\lambda,\lambda)) \\ u_2((1+\gamma)\lambda) = (u_2'((1+\gamma)\lambda)G_2((1+\gamma)\lambda,(1+\gamma)\lambda) - u_2((1+\gamma)\lambda)G_2'((1+\gamma)\lambda,(1+\gamma)\lambda)) \\ -(u_2'(\lambda)G_2(\lambda,(1+\gamma)\lambda) - u_2(\lambda)G_2'(\lambda,(1+\gamma)\lambda)) \\ u_3((1+\gamma)\lambda) = (u_3'((2+\gamma)\lambda)G_3((2+\gamma)\lambda,(1+\gamma)\lambda) - u_3((2+\gamma)\lambda)G_3'((2+\gamma)\lambda,(1+\gamma)\lambda)) - \\ -(u_3'((1+\gamma)\lambda)G_3((1+\gamma)\lambda,(1+\gamma)\lambda) - u_3((1+\gamma)\lambda)G_3'((1+\gamma)\lambda,(1+\gamma)\lambda)) \\ u_3((2+\gamma)\lambda) = (u_3'((2+\gamma)\lambda)G_3((2+\gamma)\lambda,(2+\gamma)\lambda) - u_3((2+\gamma)\lambda)G_3'((2+\gamma)\lambda,(2+\gamma)\lambda)) - \\ -(u_3'((1+\gamma)\lambda)G_3((1+\gamma)\lambda,(2+\gamma)\lambda) - u_3((1+\gamma)\lambda)G_3'((1+\gamma)\lambda,(2+\gamma)\lambda)) \end{array} \tag{D.6}$$

Boundary equations gives 6 equations with 6 unknown displacements $u_1(0), u_1(\lambda), u_2(\lambda), u_2((1+\gamma)\lambda), u_3((1+\gamma)\lambda), u_3((2+\gamma)\lambda)$ and 6 unknown slopes. In order to find solution one need 6 more equations.

In order to consider rod as the system interfacial conditions are written:

$$\begin{array}{c} u_1(\lambda) = u_2(\lambda) \\ u_1'(\lambda) = \alpha u_2'(\lambda) \\ u_2((1+\gamma)\lambda) = u_3((1+\gamma)\lambda) \\ \alpha u_2'((1+\gamma)\lambda) = u_3'((1+\gamma)\lambda) \end{array} \tag{D.7}$$

As seen, this adds only four equations. If four, five,etc. consequent cells considered, two equations still be missed. In order to get closed system for infinite rod Floquet theorem used. Floquet theorem gives possibility to transfer from finite number of cells to infinity. It statement for axial rod vibrations case can be formulated as: "displacement of two points on a distance of one period differs on a constant complex multiplier and this multiplier is constant for any cross-section". Period of structure shown on a Fig.D.1 is $(1+\gamma)\lambda$ and therefore Floquet theorem statement can be written as:

$$\begin{array}{c} u_1(0) = \Lambda u_3((1+\gamma)\lambda) \\ u_1'(0) = \Lambda u_3'((1+\gamma)\lambda) \end{array} \tag{D.8}$$

System Eq.D.6-Eq.D.8 is homogenous system of 12 equations with 12 unknown displacements and slopes. Since it homogenous, in order it to have non-trivial solution, its determinant $D(\Lambda,\Omega)$ should be zero. In this case $D(\Lambda,\Omega)$ is the second order polynomial in Λ and it can we written implicitly as (more detailed properties of this equation is considered in [15]):

$$\Lambda^2 + \frac{\Lambda\left(\alpha^2\beta^2+\sigma^2\right)\sin(\lambda\Omega)\sin\left(\frac{\gamma\lambda\Omega}{\sigma}\right)}{\alpha\beta\sigma} - 2\Lambda\cos(\lambda\Omega)\cos\left(\frac{\gamma\lambda\Omega}{\sigma}\right) + 1 = 0 \tag{D.9}$$

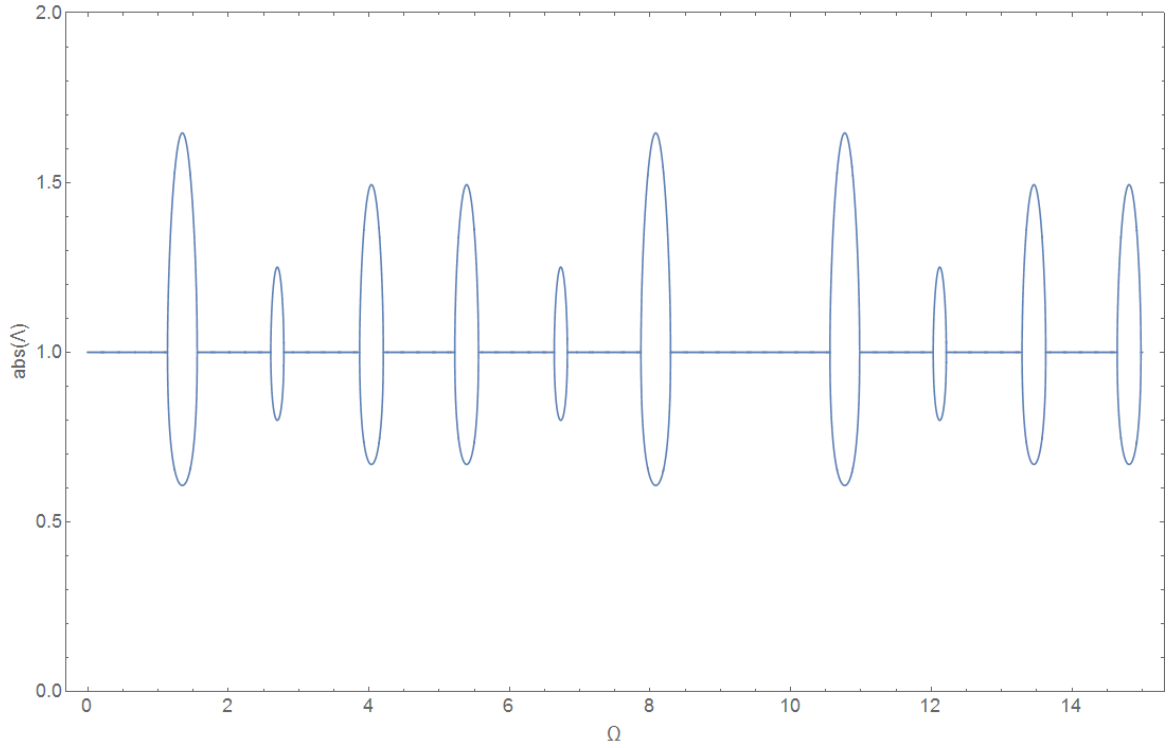

Figure D.2: Zeroes of determinant $D(\Lambda, \Omega)$ for $\alpha = 2.5\,, \beta = 1\,, \gamma = 2, \lambda = 1\,, \sigma = 1.5$

Since free term of the Eq.D.9 is 1, by Vieta's theorem there are two roots $\Lambda_i(\Omega)$, $i = 1, 2$ such that $\Lambda_1 * \Lambda_2 = 1$ and if $\text{abs}(\Lambda_1) = 1$ then $\text{abs}(\Lambda_2) = 1$. For each Ω one can plot two roots of Eq.D.9 as:

Fig.D.2 called picture of Floquet zones. It shows two kind of zones: pass band where $\text{abs}(\Lambda) = 1$ and gap bands $\text{abs}(\Lambda) \neq 1$. In pass band waves can propagate freely because amplitude of wave does not change, changes only phase. In gap band appears two standing waves with increasing and decreasing amplitude and therefore wave propagation is prohibited. Bloch proposed following form $\Lambda = \exp(iK_B)$ and K_B is called Bloch number. When K_B is purely real one have pass band and gap band otherwise. Often Floquet theorem for wave equations called also Bloch theorem, because Bloch has studied electron movement in 3D space and purposed such wave movement form as described above.